



Laboratory testing of a full scale masonry arch bridge

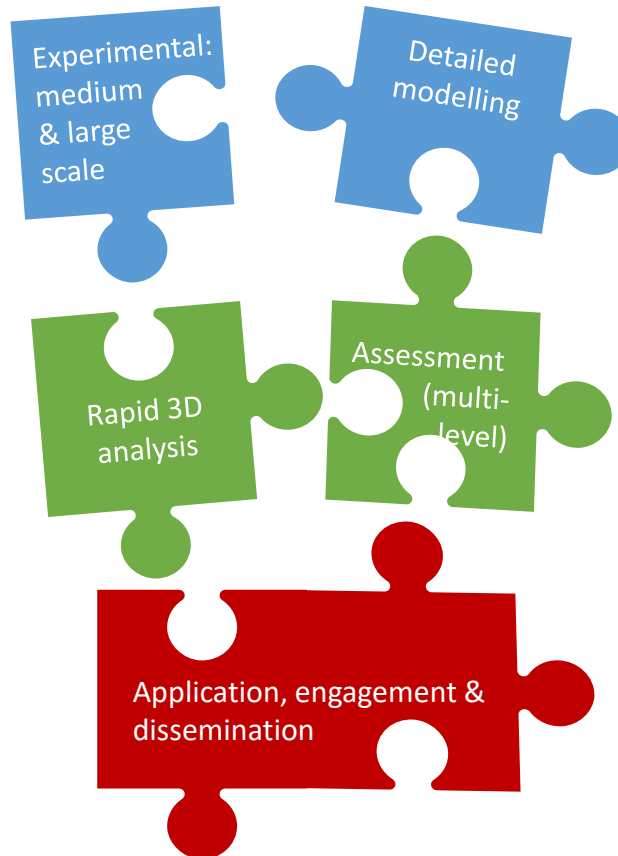
Vasilis Sarhosis

School of Civil Engineering, University of Leeds

6th September 2023



Understanding:

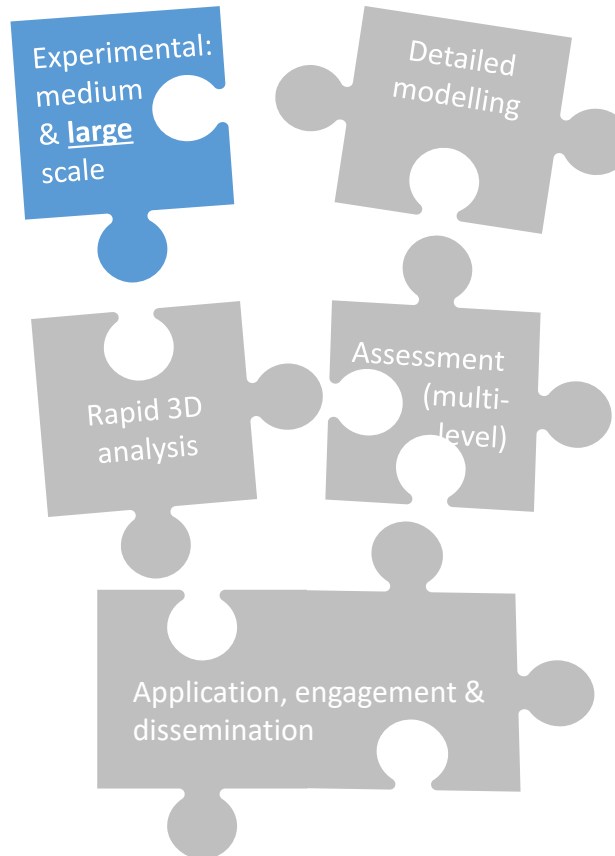


Practical tools:

Impact:



Understanding:



Practical tools:

Impact:

Principal aim: obtain an extensive experimental dataset via testing a large-scale bridge, with focus on:

- (i) 3D response,
- (ii) understand accumulation of damage and
- (iii) support development of high-fidelity models

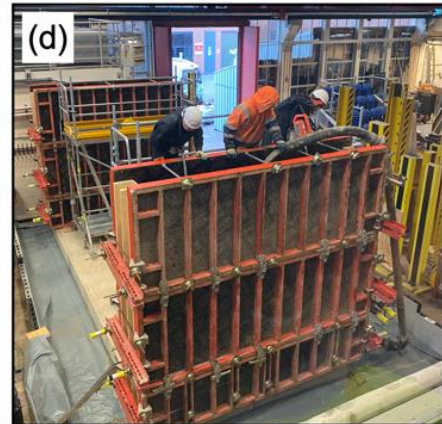
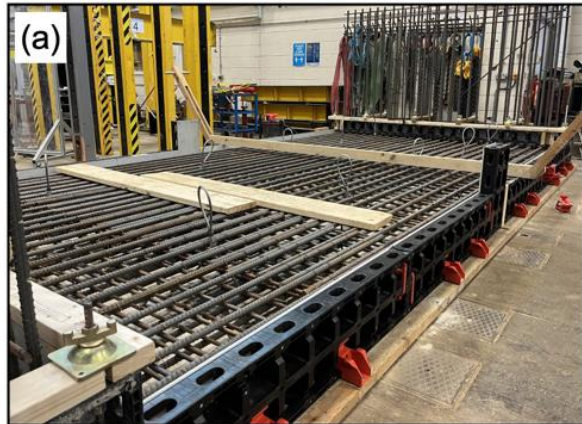
- Bridge span = 3m, with backfill and spandrels
- Bridge constructed on a stiff U-shaped RC test bed
- High strength, low water absorption bricks
- Backfill type: crushed limestone (granular)
- Loading: various point load positions / magnitudes

The George Earle Laboratory (Leeds)



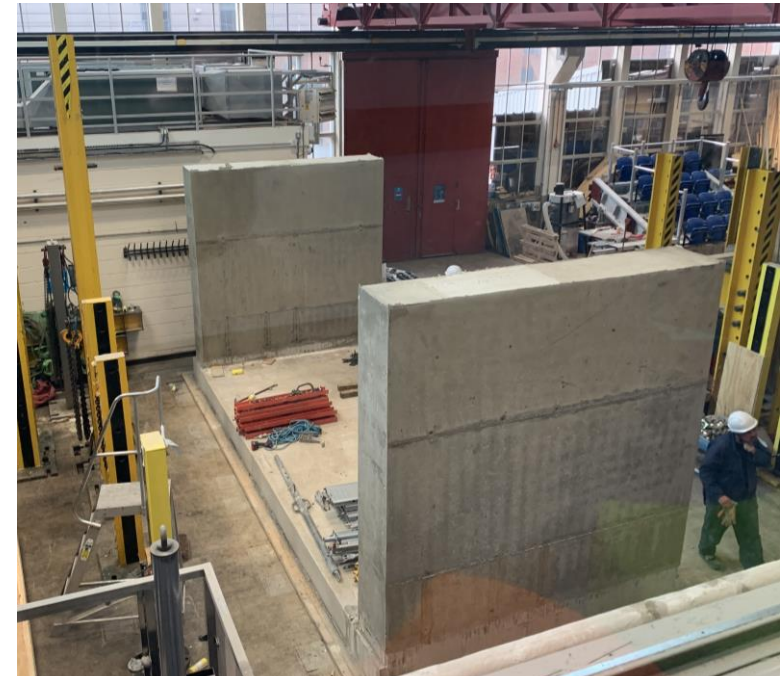
RC Strong floor with regular array of anchorage points (@ 1.55m centres) & cyclic load testing infrastructure

U-shaped RC test bed

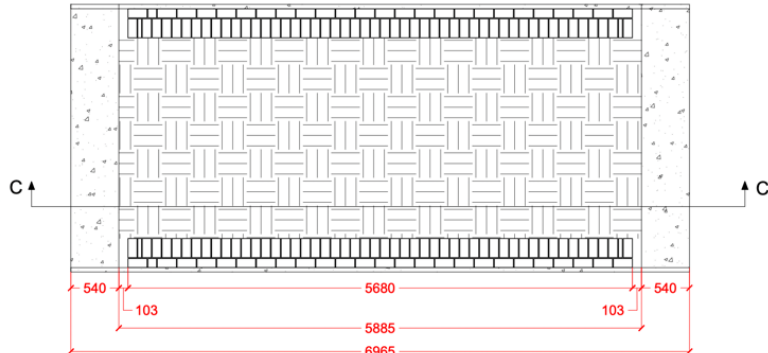


Construction of RC base slab with end walls

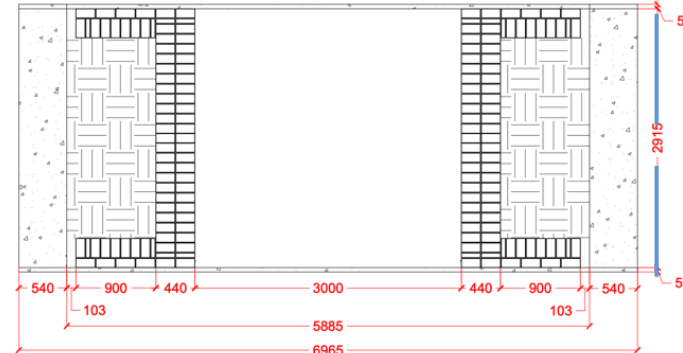
- **Dense reinforcement arrangement** adopted for the RC base slab and end walls to enhance stiffness.
- **Thickness of base slab = 300 mm;**
thickness of walls = 540 mm.
- C30-grade concrete used for construction.



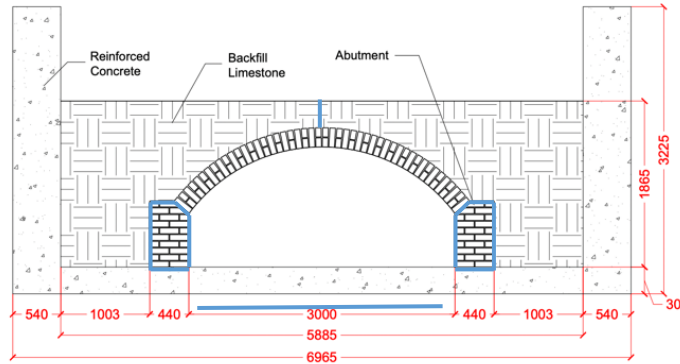
Construction Drawings



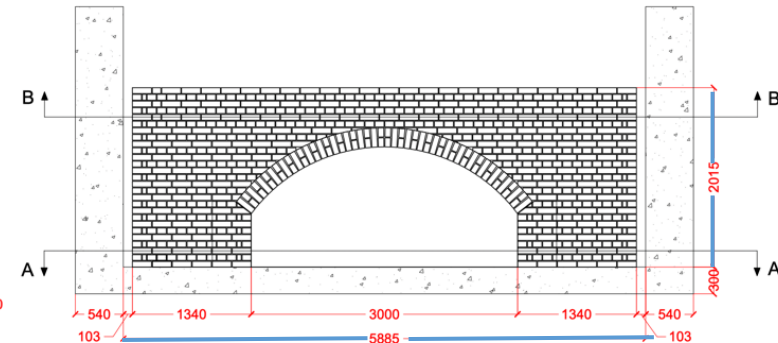
(a) Top Section B-B'



(b) Bottom Section A-A'



(c) Elevation Section C-C'



(d) Elevation

Key parameters:

- Dimensions of the bridge approx. **5.9 m length by 2 m height by 3 m width**
- Arch barrel:** 3m span single-ring header-bonded arch barrel (215 mm thickness); **4 to 1 span-to-rise ratio**
- Height of **abutment:** 600 mm (8 courses). Thickness of abutment: 440 mm (two brick thick)
- Backfill:** Crushed limestone; Backfill Depth: 300 mm over the crown of the arch barrel
- Type A** engineering bricks bonded with 10 mm thick **type O mortar** joints (OPC:Lime:Sand 1:2:9)

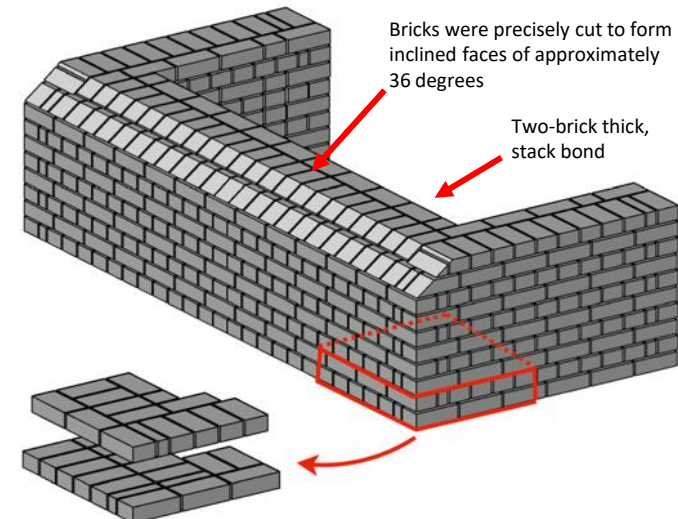
Design and construction of masonry arch bridge



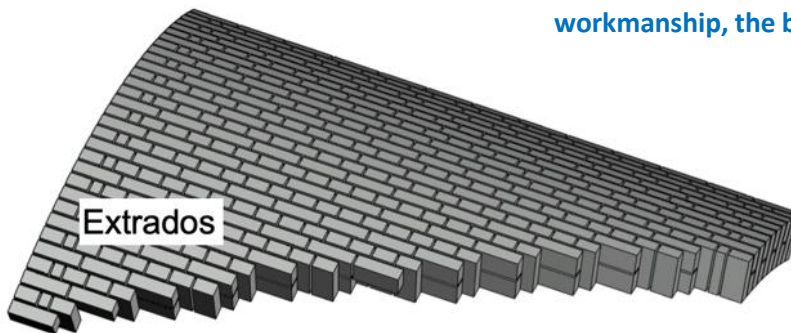
UNIVERSITY OF LEEDS



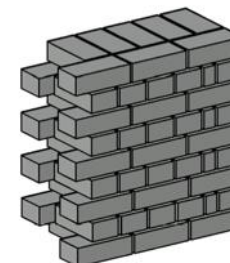
(b) Abutment and lower part of spandrel walls



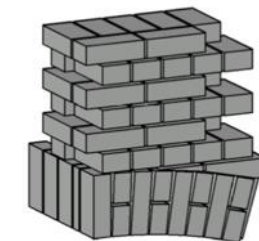
Note: to ensure consistency, and minimize variability due to workmanship, the bridge was constructed using a single bricklayer



(c) Single-ring arch barrel with a header bond (215 mm thick)



(d) One and half brick thick spandrel wall (English bond)

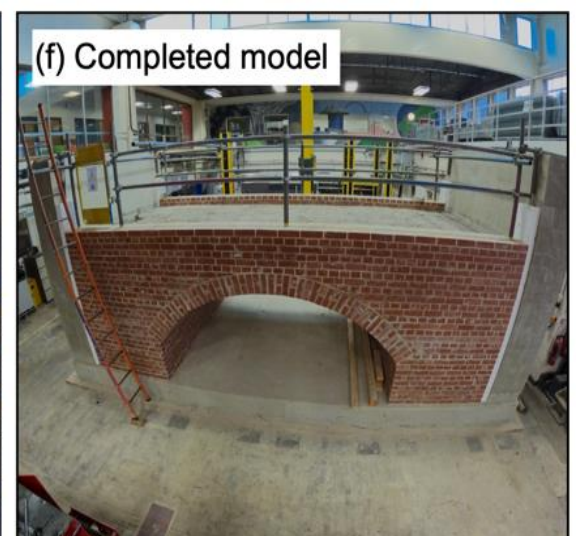


(e) Arch-spandrel wall connection

Construction process



UNIVERSITY OF LEEDS





Timelapse – Bridge construction

UNIVERSITY OF LEEDS



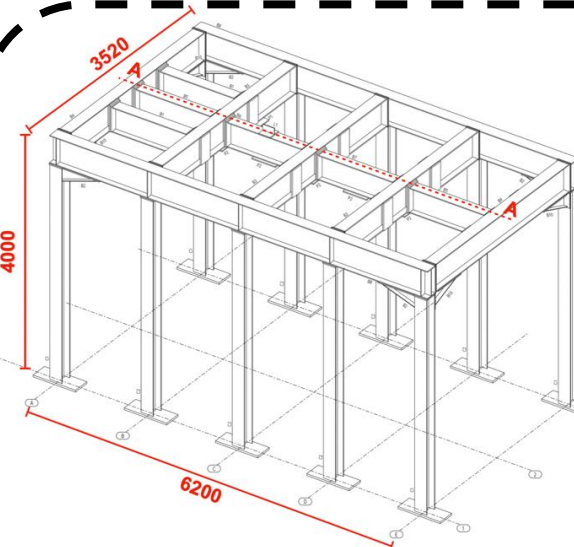


Polystyrene plates were placed at the four interior corners of the RC walls to avoid hard contact between spandrel walls and RC end walls

3D reconstruction model:

<https://sketchfab.com/3d-models/arch-bridge-state1-filtered-200k-8t8k-986bfcd08aabb463ca041fc43dd592395>

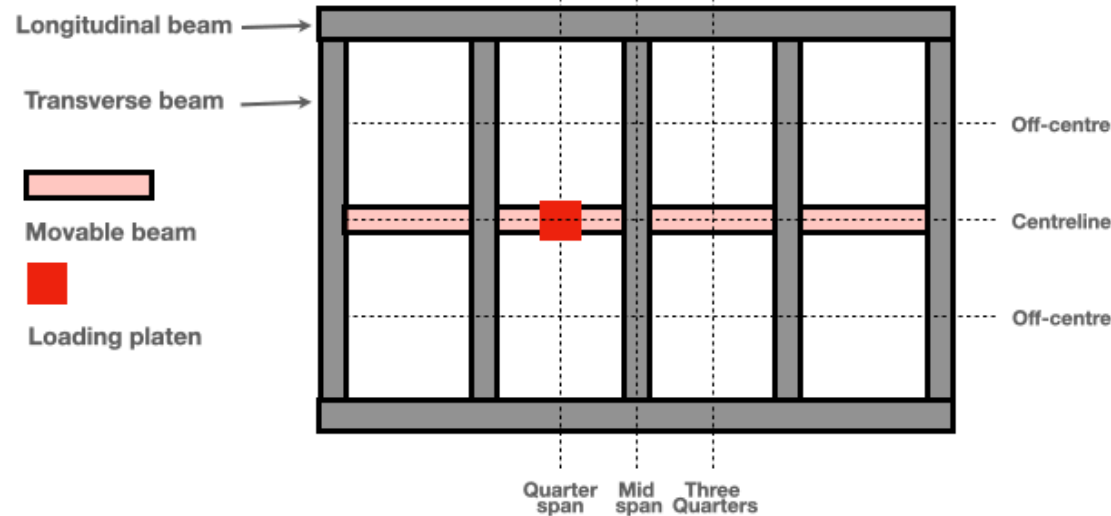
Steel reaction frame



- A steel reaction frame was specifically designed for mounting the hydraulic actuator and applying vertical static/cyclic loads

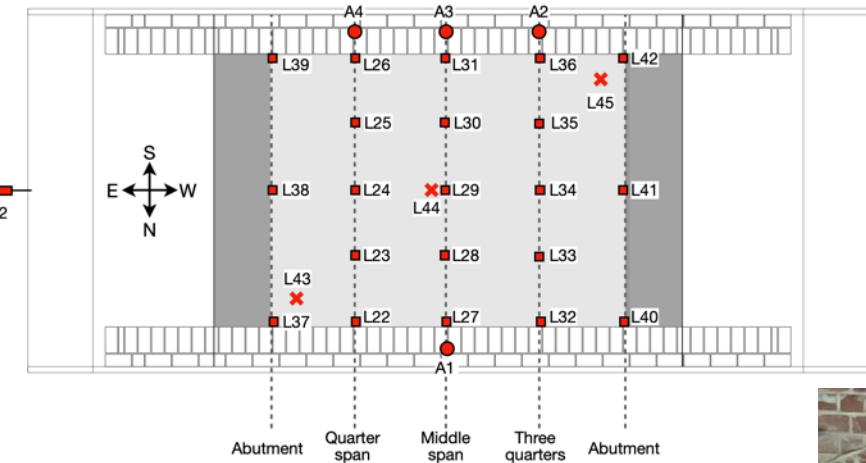
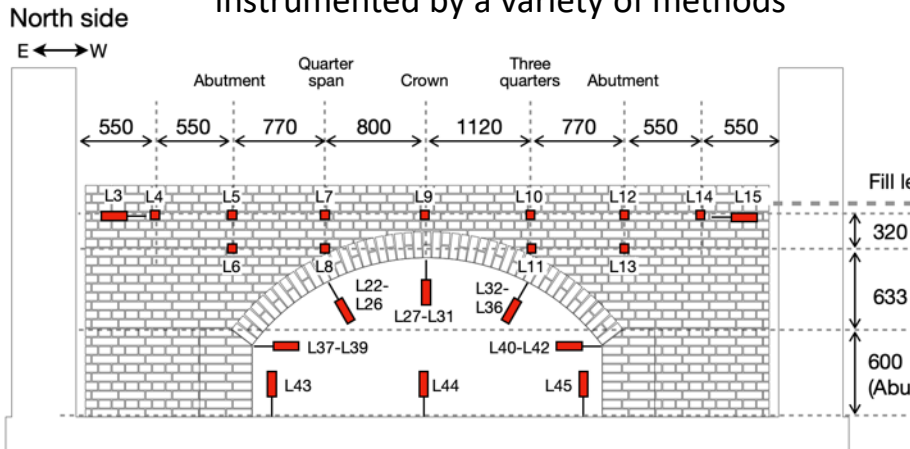


- Steel frame was rigid
- Beams and columns were steel I-sections.
- Actuators can be mounted at the short beams
- The short beams can move transversely for the application of various loading scenarios;



Instrumentation layout

- The masonry arch bridge was well instrumented by a variety of methods



| Numbers | |
|---------|------------------|
| —■— | LVDTs 46 |
| ●●— | Accelerometers 4 |

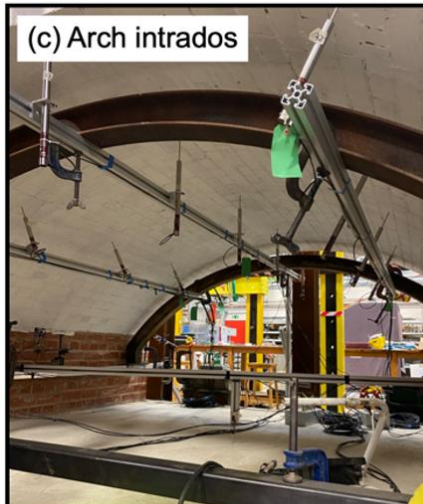
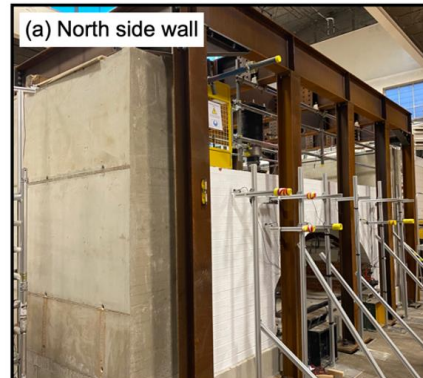


Table 1. Material and mechanical properties of bricks, mortar, masonry, and the backfill material.

| Properties | Units | No. of tests | Mean values | CV |
|--|-------------------|--------------|-------------|-------|
| Compressive strength of brick, $f_{c,u}$ | MPa | 9 | 111.3 | 6.2% |
| Young's modulus of brick, E_u | MPa | 9 | 31762 | 15.7% |
| Tensile strength of brick, $f_{t,u}$ | MPa | 9 | 6.730 | 13.5% |
| Brick density, ρ_u | kg/m ³ | 9 | 2470 | 1.3% |
| Flexural strength of mortar, $f_{b,j}$ | MPa | 20 | 0.627 | 20.9% |
| Compressive strength of mortar, $f_{c,j}$ | MPa | 40 | 1.736 | 25.7% |
| Young's modulus of mortar, E_j | MPa | 40 | 128.6 | 35.3% |
| Mortar density, ρ_j | kg/m ³ | 20 | 1680 | 2.3% |
| Friction angle at brick-to-mortar interface, φ | Degree | 3 | 44.9 | - |
| Cohesion at brick-to-mortar interface, C | MPa | 3 | 0.40 | - |
| Compressive strength of masonry, $f_{c,m}$ | MPa | 3 | 30.84 | 24.2% |
| Young's modulus of masonry, E_m | MPa | 3 | 10128 | 48.4% |
| Friction angle of limestone, φ_b | Degree | 6 | 47.8 | - |
| Limestone density (bulk), ρ_b | kg/m ³ | - | 2150 | - |

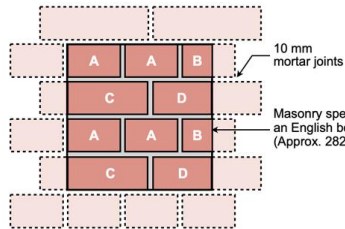


Small-scale testing for material characterisation

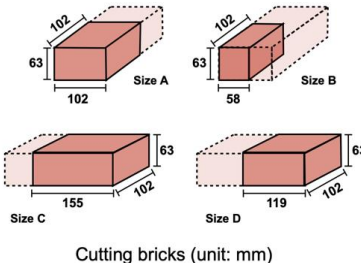
(a) three-point bending tests on mortar prisms; (b) compression tests on mortar cubes; (c) compression tests on bricks; (d) Brazilian tests on brick cylinders; (e) triplet shear tests; (f) compression tests on masonry prisms.

- All specimens constructed at the same time as the construction of the masonry arch bridge, and tested at the time of testing the bridge i.e. same curing conditions.
- Designed in close association with colleagues developing numerical models

(a) Spandrel wall-to-backfill interface

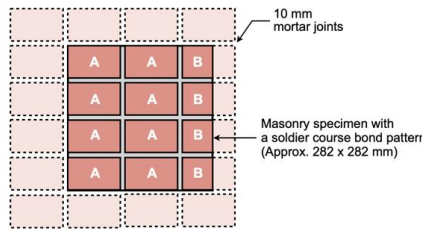


Masonry with an English bond pattern

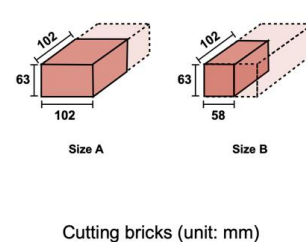


Brickwork specimen with an English bond pattern

(b) Arch-to-backfill interface

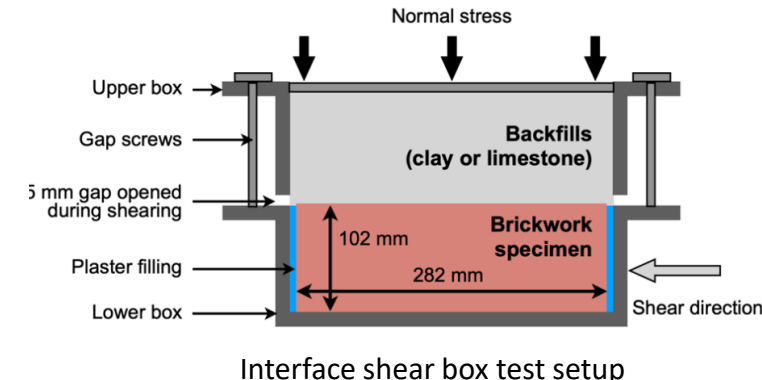


Masonry with a soldier course bond pattern



Brickwork specimen with a soldier course bond pattern

Design of masonry specimens



Interface shear box test setup

More info, please refer to :

- Liu et al. 2023. *Construction and Building Materials*, 397, <https://doi.org/10.1016/j.conbuildmat.2023.132347>.
- Liu et al. 2023. *Engineering Structures*, 292, <https://doi.org/10.1016/j.engstruct.2023.116531>.

| Samples/interfaces | Friction angle (°) | Cohesion (kPa) | R ² | φ_i/φ |
|--------------------|--------------------|----------------|----------------|---------------------|
| Clay | 37.2 | 30.0 | 0.950 | - |
| Limestone | 47.8 | 0 | 0.994 | - |
| EC interface | With cohesion | 14.5 | 0.942 | 0.39 |
| | Zero-cohesion | 19.2 | 0.993 | 0.52 |
| SC interface | With cohesion | 12.9 | 0.967 | 0.35 |
| | Zero-cohesion | 18.9 | 0.991 | 0.51 |
| EL interface | 33.3 | 0 | 0.994 | 0.70 |
| SL interface | 35.7 | 0 | 0.999 | 0.75 |

9 loading locations (point A to point I)

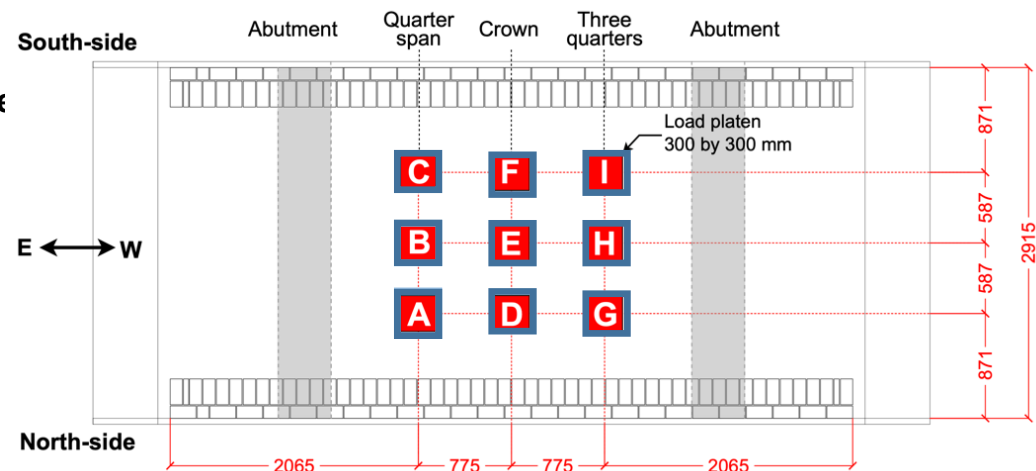
First load was quasi-static, then 3 quasi-static cycles

- Low-level: 150 kN (elastic limit)
- **Mid-level: 250 kN (less than 50% of ULS)**
- **High-level: 560 kN;**
- **Failure-level tests: until failure**

Specification for the loading area

300 by 300 mm for the low- and mid-level

300 by 750 mm for the high-level and ultimate



| Location | Testing sequence → | | | | | | | | | | | | | | | | | | | | | | | | | |
|----------|--------------------|----|----|----|----|----|----|----|----|-----|-----|-----|-----|-----|-----|-----|-----|-----|-----|-----|-----|-----|-----|-----|-----|--|
| | T1 | T2 | T3 | T4 | T5 | T6 | T7 | T8 | T9 | T10 | T11 | T12 | T13 | T14 | T15 | T16 | T17 | T18 | T19 | T20 | T21 | T22 | T23 | T24 | T25 | |
| A | ■ | | | | | | ■ | | | | | | ■ | ■ | | | | | | | | | | | | |
| B | | ■ | | | | | | ■ | ■ | | | | | | | | | | | | | | | | | |
| C | | | ■ | ■ | | | | | | | | | | | | | | | | | | | | | | |
| D | | | | ■ | ■ | | | | | | | | ■ | ■ | | | | | | | | | | | | |
| E | | | | | ■ | ■ | | | | | | | | | | | | | | | | | | | | |
| F | | | | | | ■ | ■ | | | | | | ■ | ■ | | | | | | | | | | | | |
| G | | | | | | | | ■ | ■ | | | | ■ | ■ | | | | | | | | | | | | |
| H | | | | | | | | | ■ | ■ | | | | ■ | ■ | | | | | | | | | | | |
| I | | | | | | | | | | ■ | ■ | | | | | | | | | | | | | | | |

■ Low-level static

■ Low-level three cycles

■ Mid-level static

■ Mid-level three cycles

■ High-level static

■ Failure-level static

9 loading locations (point A to point I)

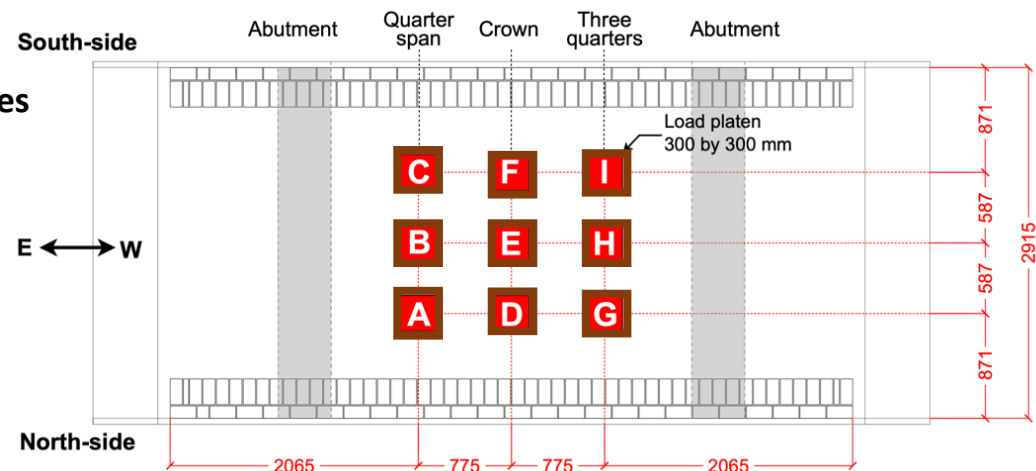
First load was quasi-static, then 3 quasi-static cycles

- **Low-level:** 150 kN (elastic limit)
- **Mid-level:** 250 kN (less than 50% of ULS)
- **High-level:** 560 kN
- **Failure-level tests:** until failure

Specification for the loading area

300 by 300 mm for the low- and mid-level

300 by 750 mm for the high-level and ultimate



| Location | Testing sequence → | | | | | | | | | | | | | | | | | | | | | | | | | |
|----------|--------------------|----|----|----|----|----|----|----|----|-----|-----|-----|-----|-----|-----|-----|-----|-----|-----|-----|-----|-----|-----|-----|-----|--|
| | T1 | T2 | T3 | T4 | T5 | T6 | T7 | T8 | T9 | T10 | T11 | T12 | T13 | T14 | T15 | T16 | T17 | T18 | T19 | T20 | T21 | T22 | T23 | T24 | T25 | |
| A | ■ | | | | | | ■ | | | | | | ■ | ■ | | | | | | | | | | | | |
| B | | ■ | | | | | | ■ | ■ | | | | | | | | | | | | | | | | | |
| C | | | ■ | ■ | | | | | | | | | | | | | | | | | | | | | | |
| D | | | | ■ | ■ | | | | | | | | ■ | ■ | | | | | | | | | | | | |
| E | | | | | ■ | ■ | | | | | | | | | | | | | | | | | | | | |
| F | | | | | | ■ | ■ | | | | | | ■ | ■ | | | | | | | | | | | | |
| G | | | | | | | | ■ | ■ | | | | ■ | ■ | | | | | | | | | | | | |
| H | | | | | | | | | ■ | ■ | | | | ■ | ■ | | | | | | | | | | | |
| I | | | | | | | | | | ■ | ■ | | | | | | | | | | | | | | | |

■ Low-level static

■ Low-level three cycles

■ Mid-level static

■ Mid-level three cycles

■ High-level static

■ Failure-level static

9 loading locations (point A to point I)

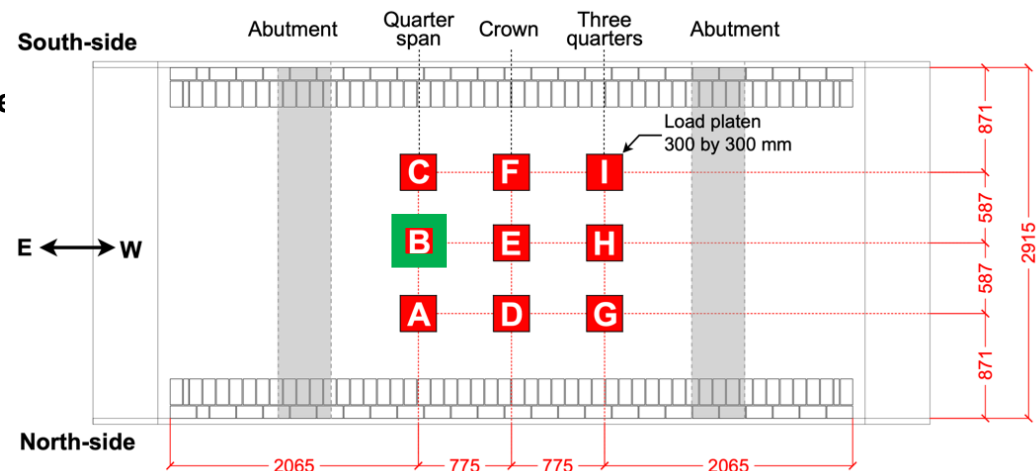
First load was quasi-static, then 3 quasi-static cycles

- **Low-level:** 150 kN (elastic limit)
- **Mid-level:** 250 kN (less than 50% of ULS)
- **High-level:** 560 kN
- **Failure-level tests:** until failure

Specification for the loading area

300 by 300 mm for the low- and mid-level

300 by 750 mm for the high-level and ultimate



| Location | Testing sequence → | | | | | | | | | | | | | | | | | | | | | | | | | |
|----------|--------------------|----|----|----|----|----|----|----|----|-----|-----|-----|-----|-----|-----|-----|-----|-----|-----|-----|-----|-----|-----|-----|-----|--|
| | T1 | T2 | T3 | T4 | T5 | T6 | T7 | T8 | T9 | T10 | T11 | T12 | T13 | T14 | T15 | T16 | T17 | T18 | T19 | T20 | T21 | T22 | T23 | T24 | T25 | |
| A | ■ | | | | | | ■ | | | | | | | | | | | | | | | | | | | |
| B | | ■ | | | | | | ■ | ■ | | | | | | | | | | | | | | | | | |
| C | | | ■ | ■ | | | | | | | | | | | | | | | | | | | | | | |
| D | | | | ■ | ■ | | | | | | | | | | | | ■ | | | | | | | | | |
| E | | | | | ■ | ■ | | | | | | | | | | | | | | | | | | | | |
| F | | | | | | ■ | ■ | | | | | | | | | | | | | | | | | | | |
| G | | | | | | | | ■ | ■ | | | | | | | | | | | | | | | | | |
| H | | | | | | | | | ■ | ■ | | | | | | | | | | | | | | | | |
| I | | | | | | | | | | ■ | ■ | | | | | | | | | | | | | | | |

■ Low-level static

■ Low-level three cycles

■ Mid-level static

■ Mid-level three cycles

■ High-level static

■ Failure-level static

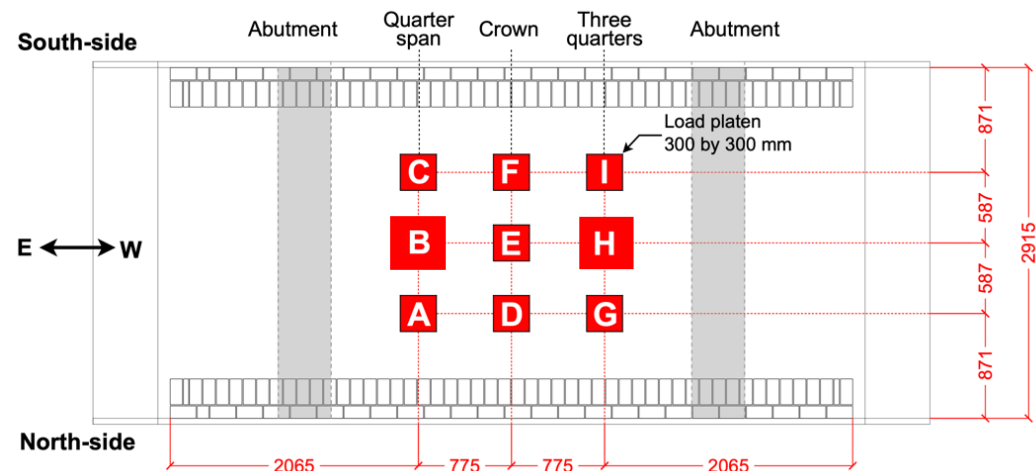
9 loading locations (point A to point I)

- **Low-level:** 150 kN (elastic limit)
- **Mid-level:** 250 kN (less than 50% of ULS,
- **High-level:** 560 kN;
- **Failure-level tests: until failure**

Specification for the loading area

300 by 300 mm for the low- and mid-level

300 by 750 mm for the high-level and ultimate



| Location | Testing sequence → | | | | | | | | | | | | | | | | | | | | | | | | | |
|----------|--------------------|----|----|----|----|----|----|----|----|-----|-----|-----|-----|-----|-----|-----|-----|-----|-----|-----|-----|-----|-----|-----|-----|--|
| | T1 | T2 | T3 | T4 | T5 | T6 | T7 | T8 | T9 | T10 | T11 | T12 | T13 | T14 | T15 | T16 | T17 | T18 | T19 | T20 | T21 | T22 | T23 | T24 | T25 | |
| A | ■ | | | | | | ■ | | | | | | | | | | | | | | | | | | | |
| B | | ■ | | | | | | ■ | ■ | | | | | | | | | | | | | | | | | |
| C | | | ■ | ■ | | | | | | | | | | | | | | | | | | | | | | |
| D | | | | ■ | ■ | | | | | | | | | | | | ■ | ■ | | | | | | | | |
| E | | | | | ■ | ■ | | | | | | | | | | | | | | | | | | | | |
| F | | | | | | ■ | ■ | | | | | | | | | | | | | | | | | | | |
| G | | | | | | | | ■ | ■ | | | | | | | | | | | | | | | | | |
| H | | | | | | | | | ■ | ■ | | | | | | | | | | | | | | | | |
| I | | | | | | | | | | ■ | ■ | | | | | | | | | | | | | | | |

■ Low-level static

■ Low-level three cycles

■ Mid-level static

■ Mid-level three cycles

■ High-level static

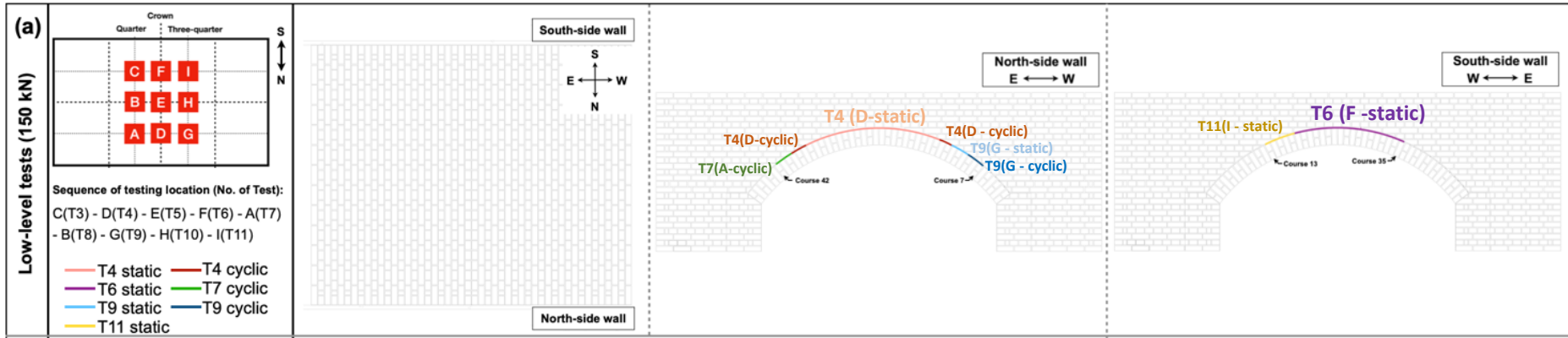
■ Failure-level static

Results: Crack propagation – damage evolution

Arch intrados

North side

South side



Low-level: 150 kN

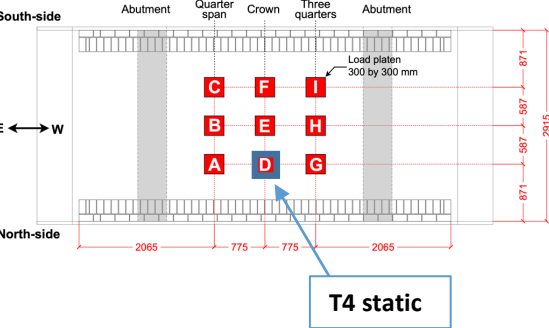
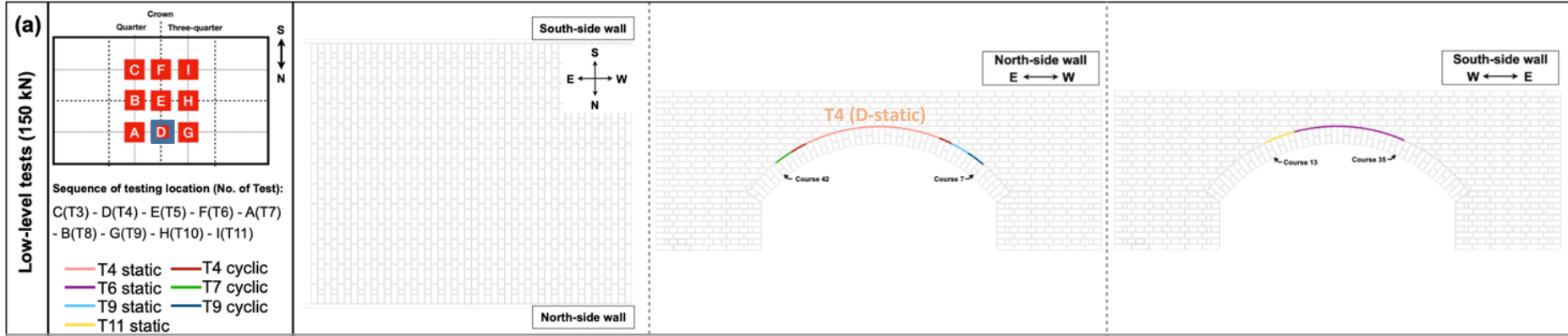
- At low level of loads, cracks were very thin (hairline cracks).
- With the removal of the load, cracks closed.
- First crack observed when load applied at the crown close to the spandrel wall (Point D).
- The first crack was a detachment of the arch ring from the spandrel wall.

Results: Crack propagation – damage evolution

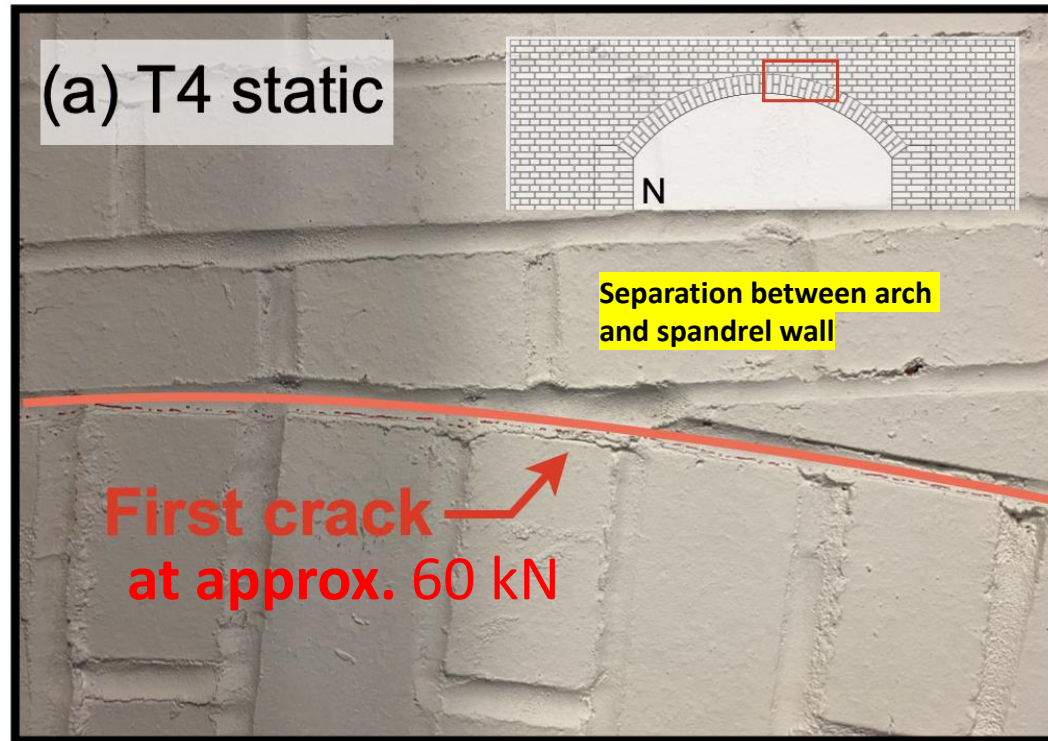
Arch intrados

North side

South side



Low-level: 150 kN

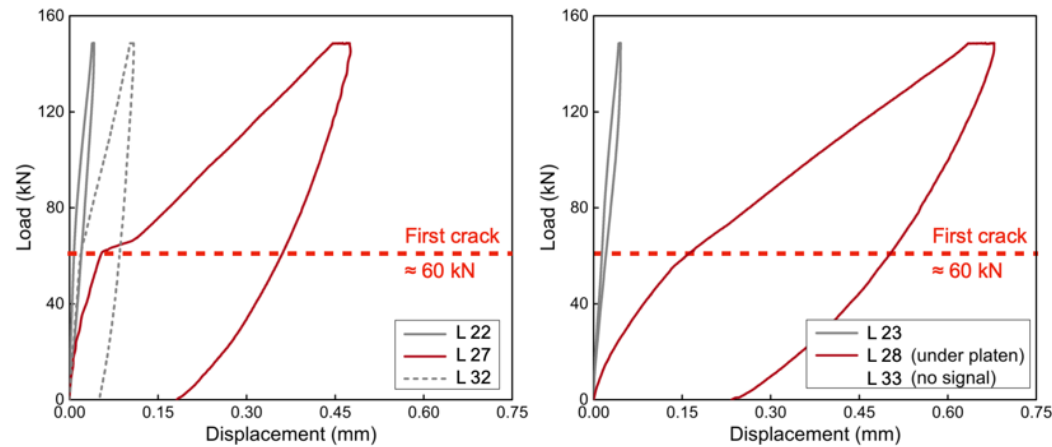
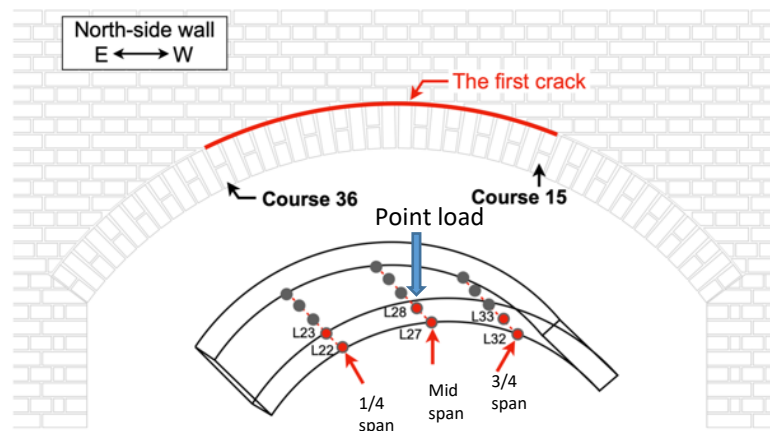
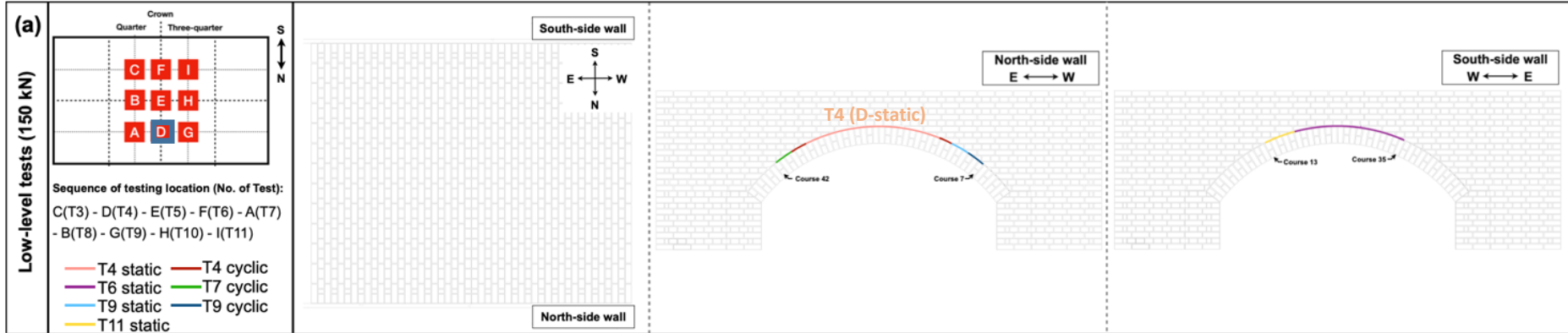


Results: Crack propagation – damage evolution

Arch intrados

North side

South side



- **The first crack:** separation between the arch barrel and spandrel wall
- **Loading location:** Point D
- **Cracking load:** approximately 60 kN

Displacement close to the edge of the arch ring (L27)

Displacement under point load (L28)

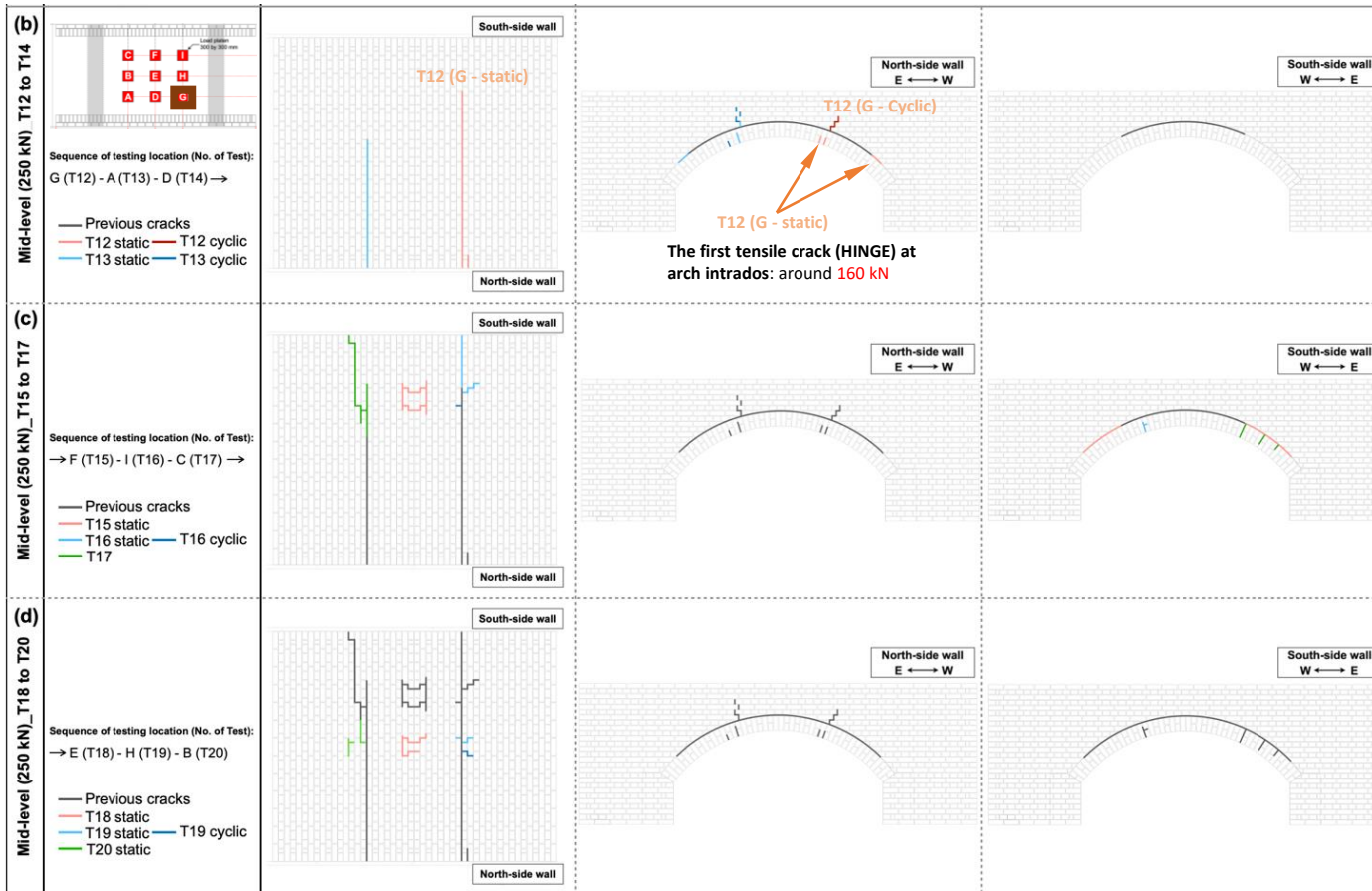
Results: Crack propagation – damage evolution

Arch intrados

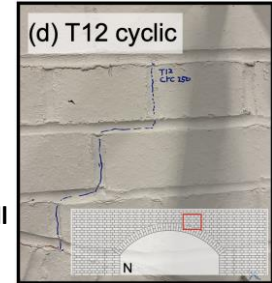
North side

South side

- Mid-level: 250 kN (less than 50% of ULS)



Diagonal crack
at spandrel wall
(G location)



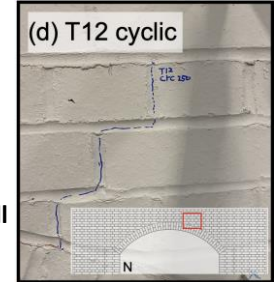
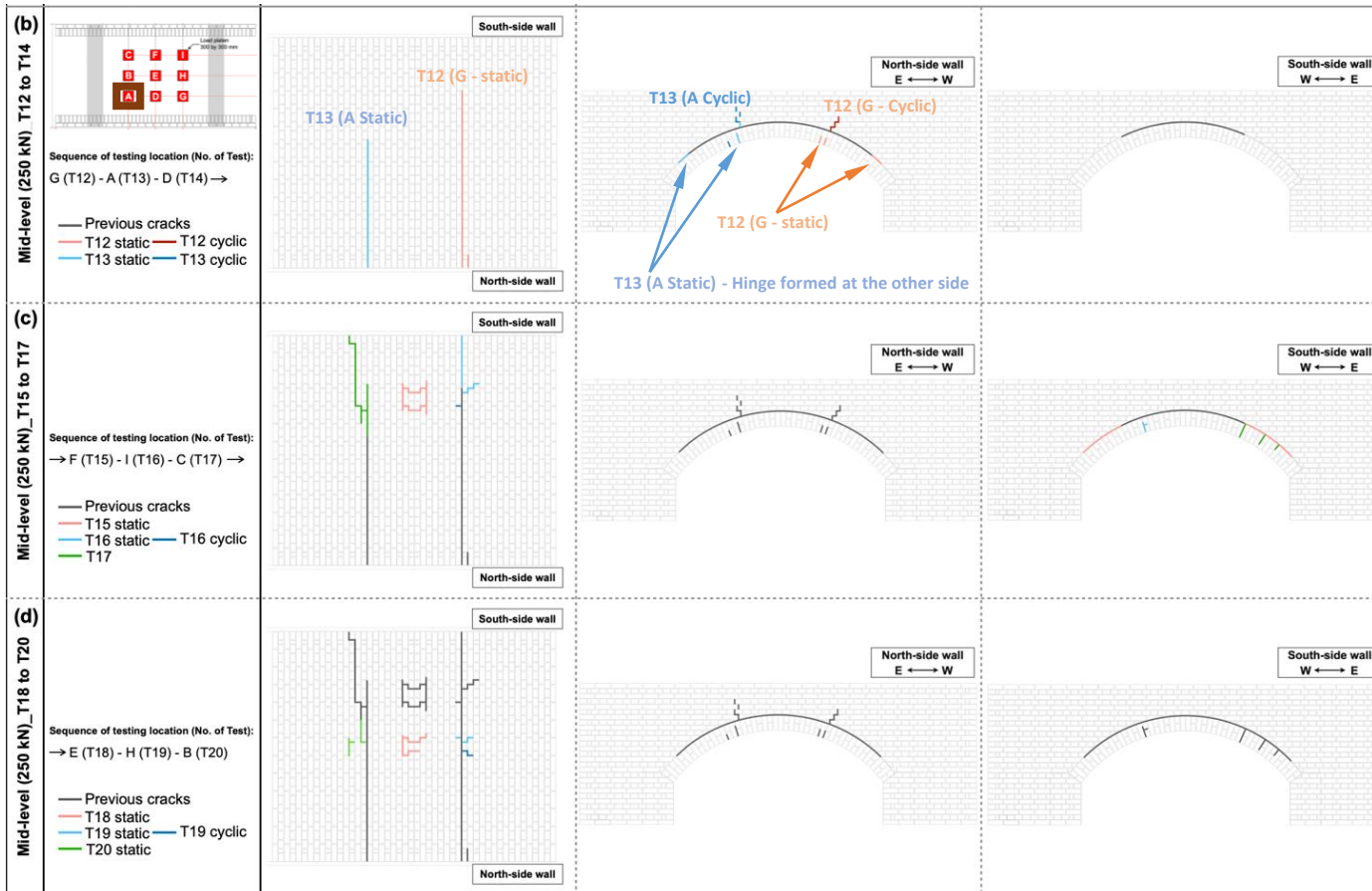
Results: Crack propagation – damage evolution

Arch intrados

North side

South side

- Mid-level: 250 kN (less than 50% of ULS)



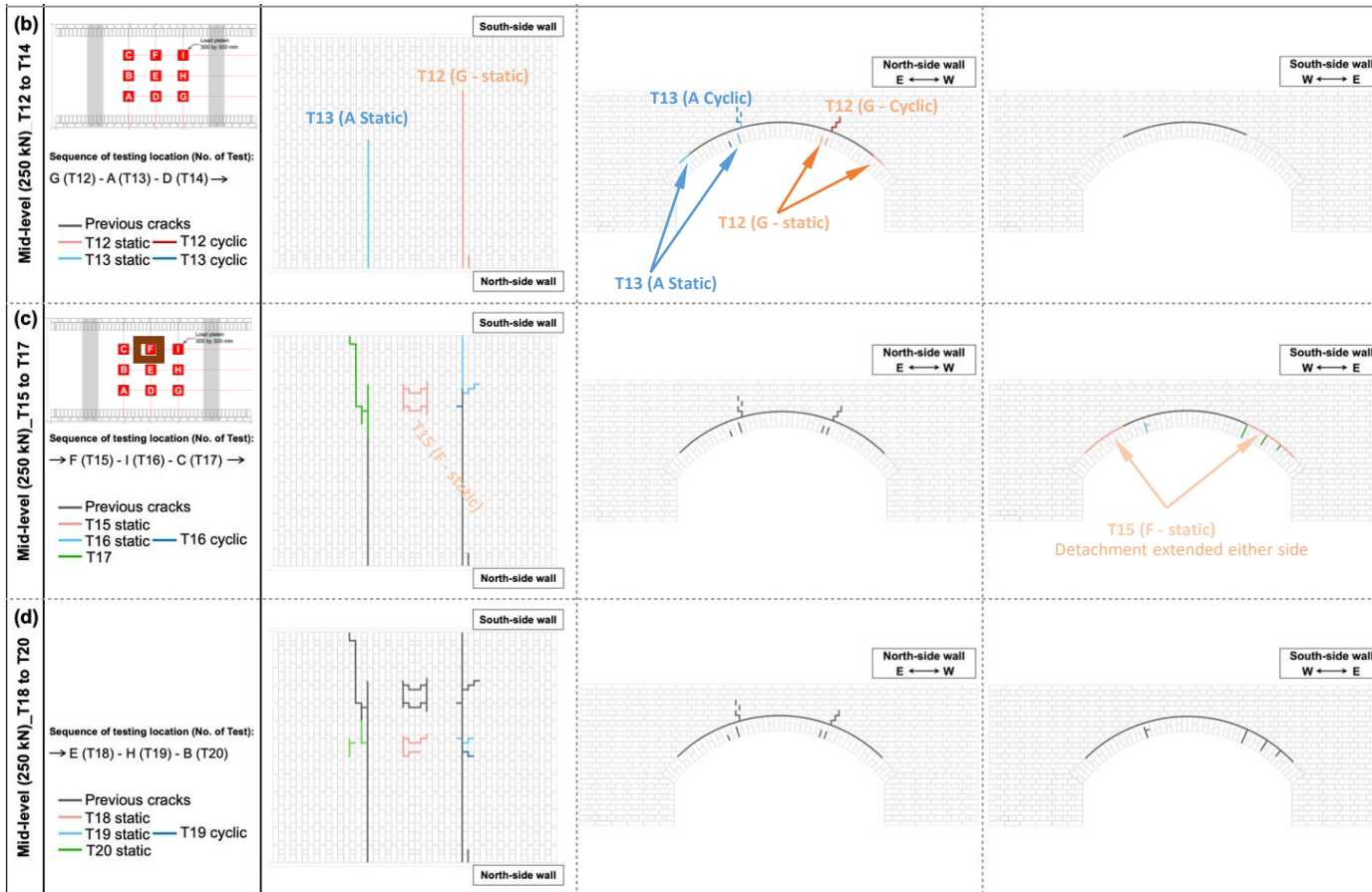
Results: Crack propagation – damage evolution

Arch intrados

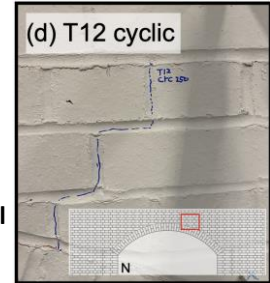
North side

South side

- Mid-level: 250 kN (less than 50% of ULS)



Diagonal crack
at spandrel wall
(G location)



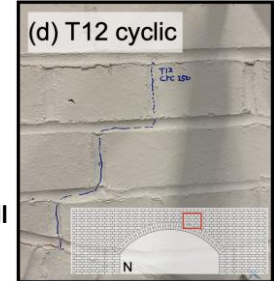
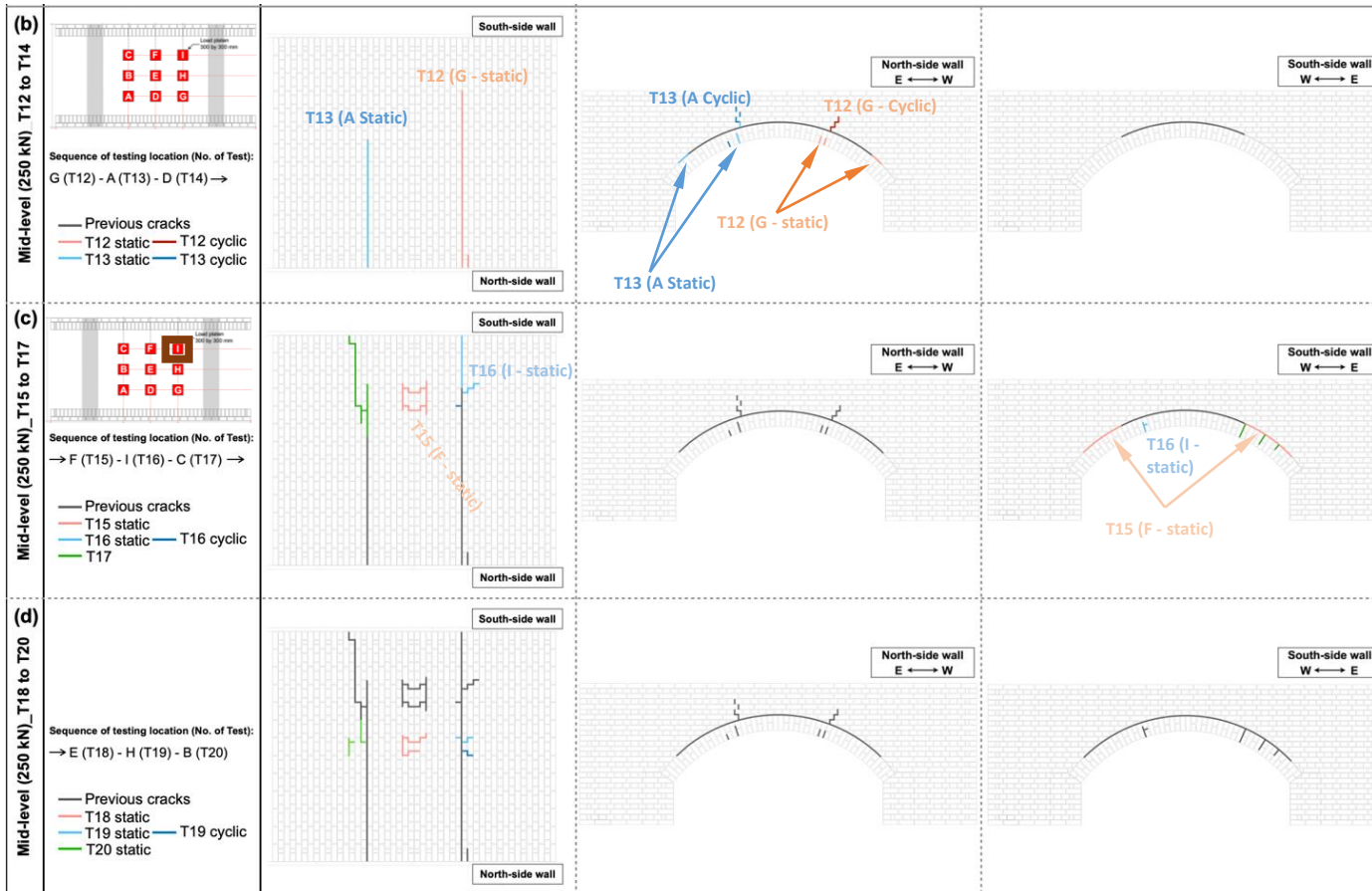
Results: Crack propagation – damage evolution

Arch intrados

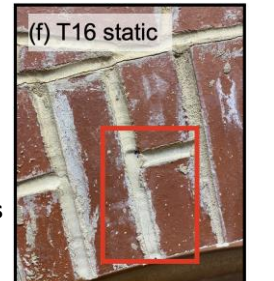
North side

South side

- Mid-level: 250 kN (less than 50% of ULS)



Diagonal crack
at spandrel wall
(G location)



Tensile crack
at arch intrados

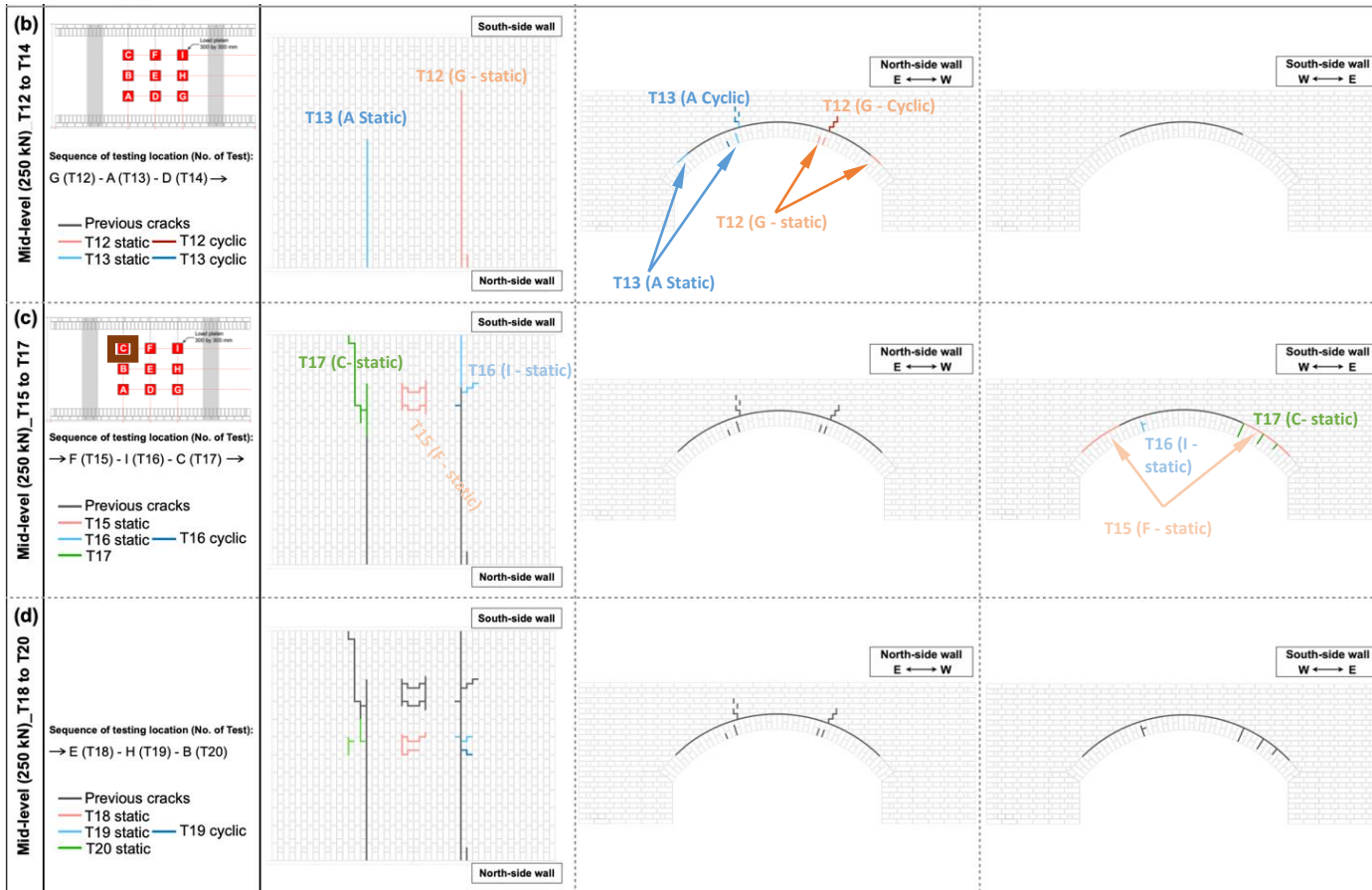
Results: Crack propagation – damage evolution

Arch intrados

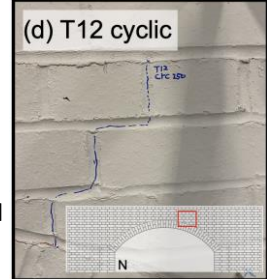
North side

South side

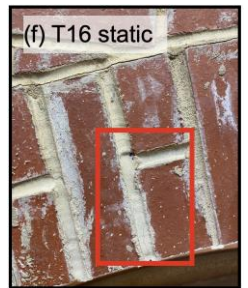
- Mid-level: 250 kN (less than 50% of ULS)



Diagonal crack at spandrel wall (G location)



Tensile crack at arch intrados



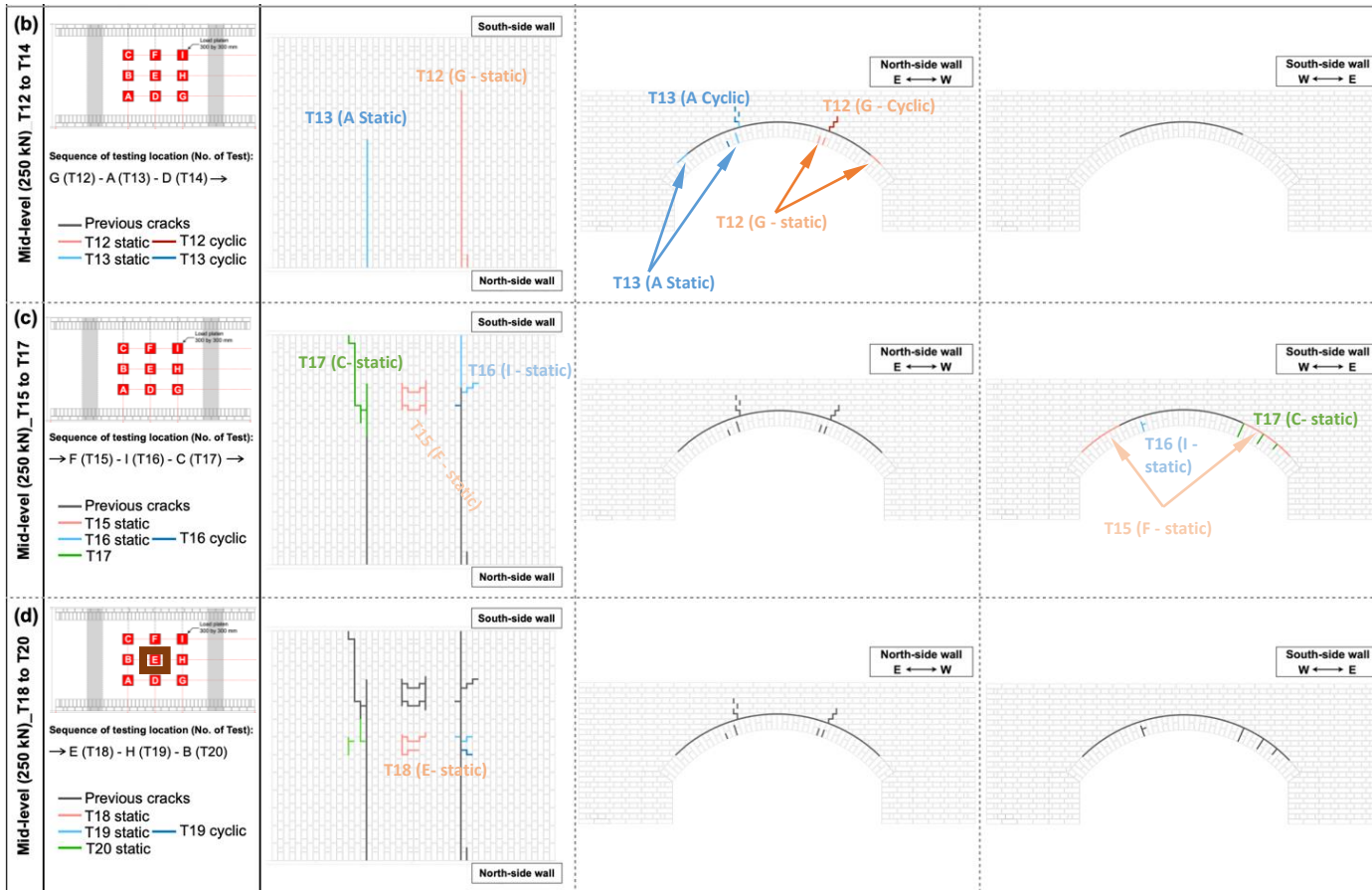
Results: Crack propagation – damage evolution

Arch intrados

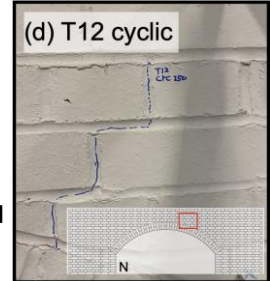
North side

South side

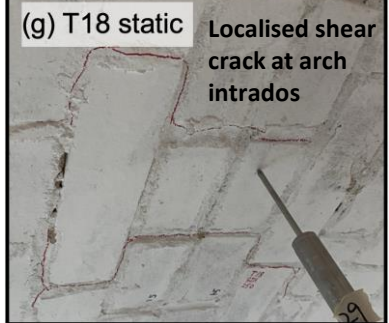
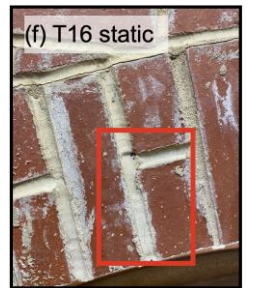
- Mid-level: 250 kN (less than 50% of ULS)



Diagonal crack at spandrel wall (G location)



Tensile crack at arch intrados



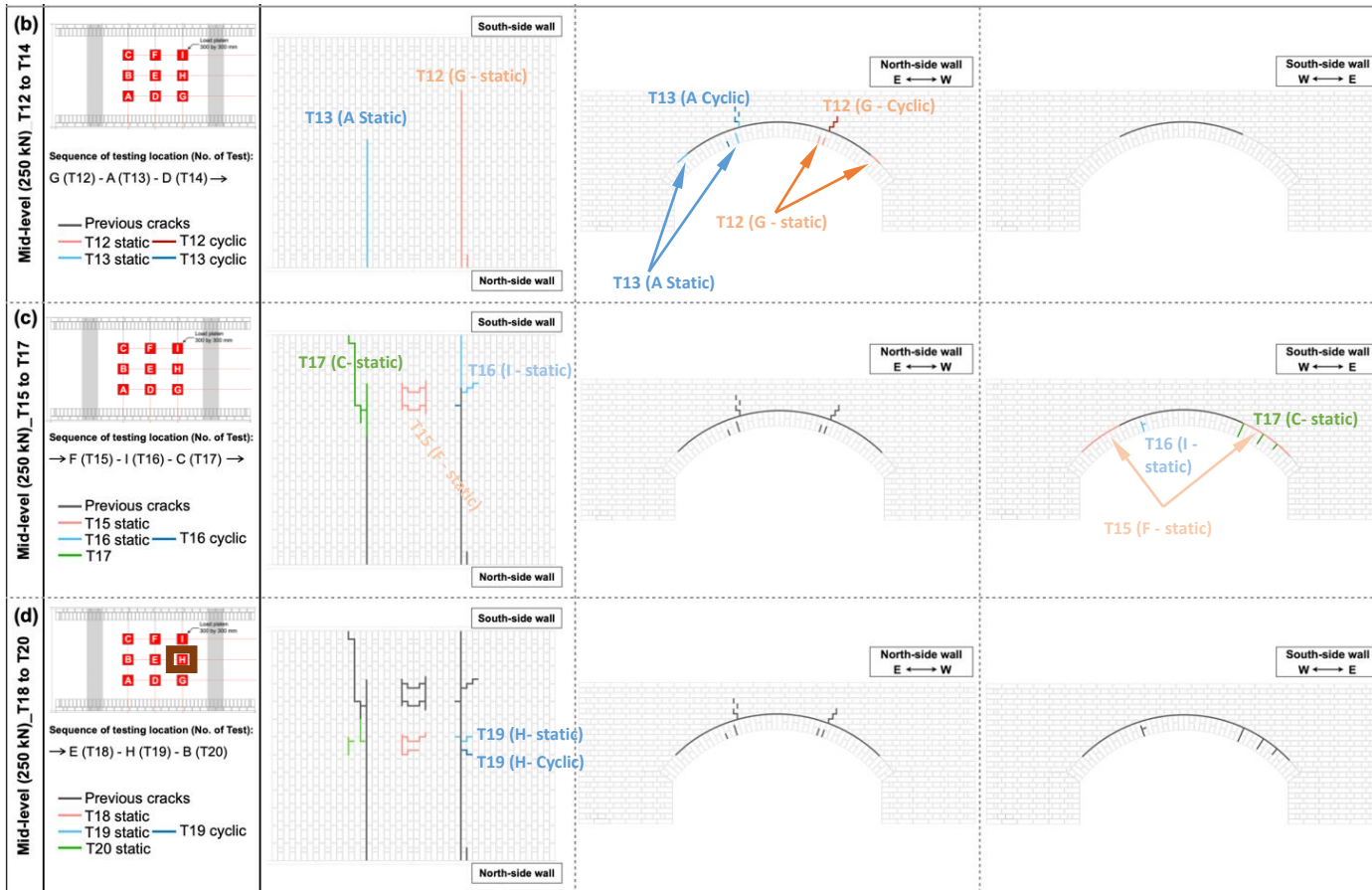
Results: Crack propagation – damage evolution

Arch intrados

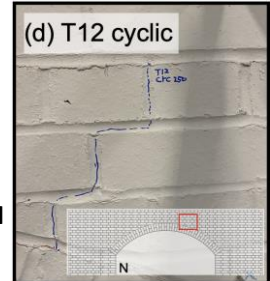
North side

South side

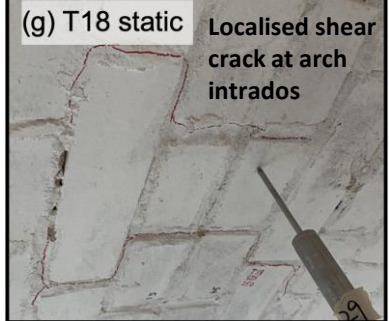
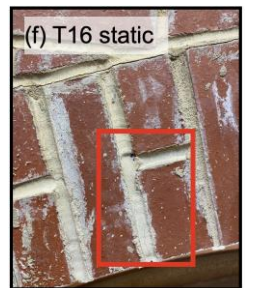
- Mid-level: 250 kN (less than 50% of ULS)



Diagonal crack at spandrel wall (G location)



Tensile crack at arch intrados



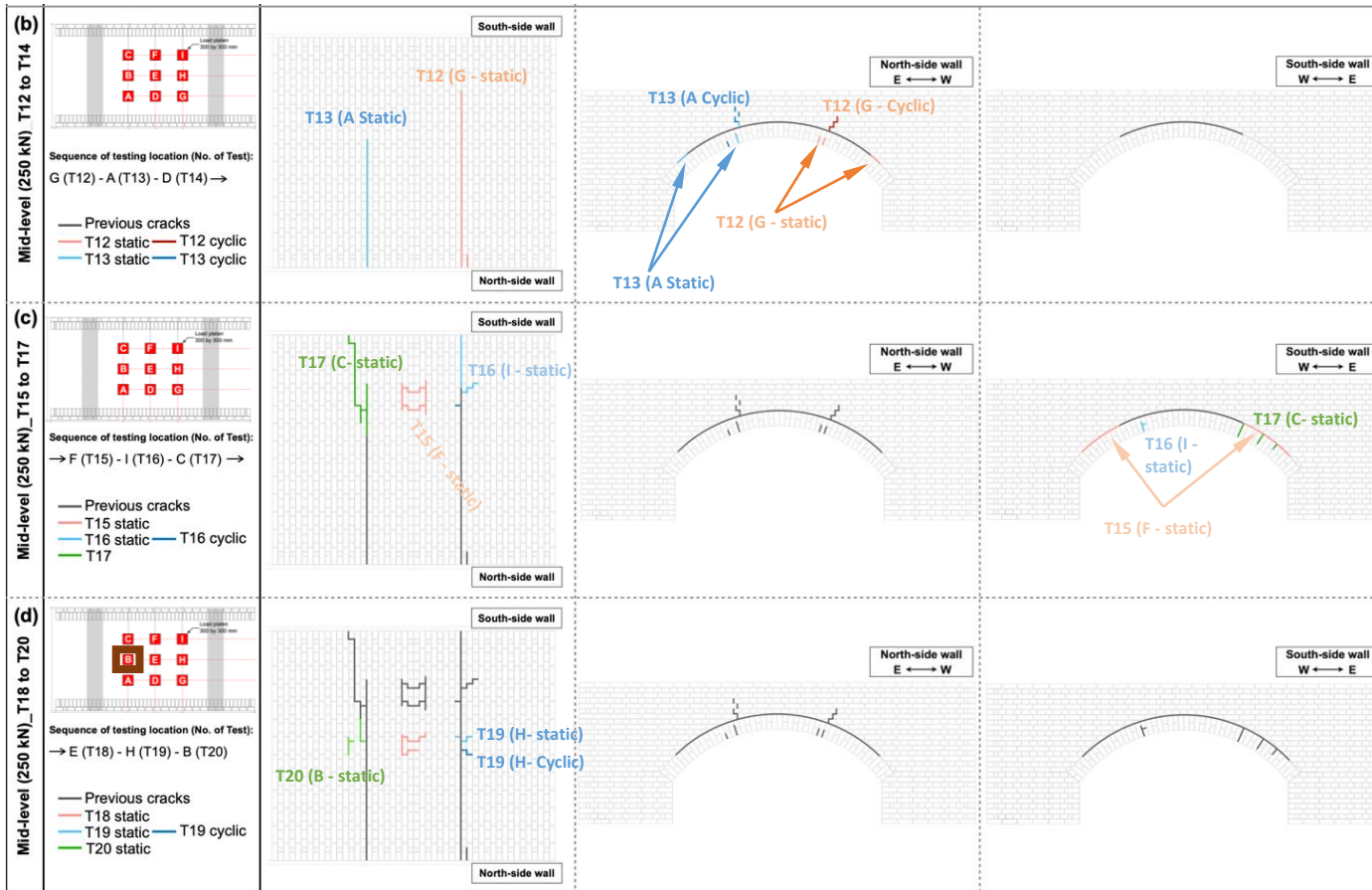
Results: Crack propagation – damage evolution

Arch intrados

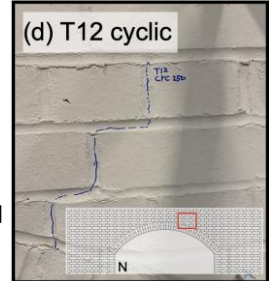
North side

South side

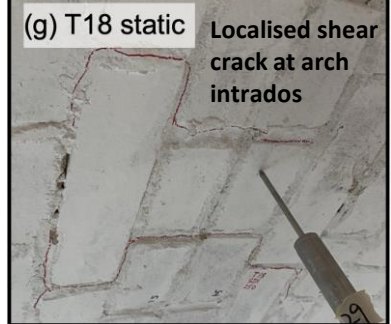
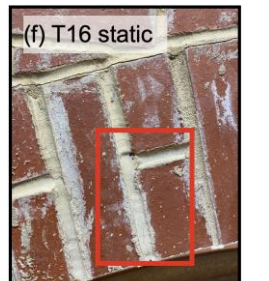
- Mid-level: 250 kN (less than 50% of ULS)



Diagonal crack at spandrel wall (G location)

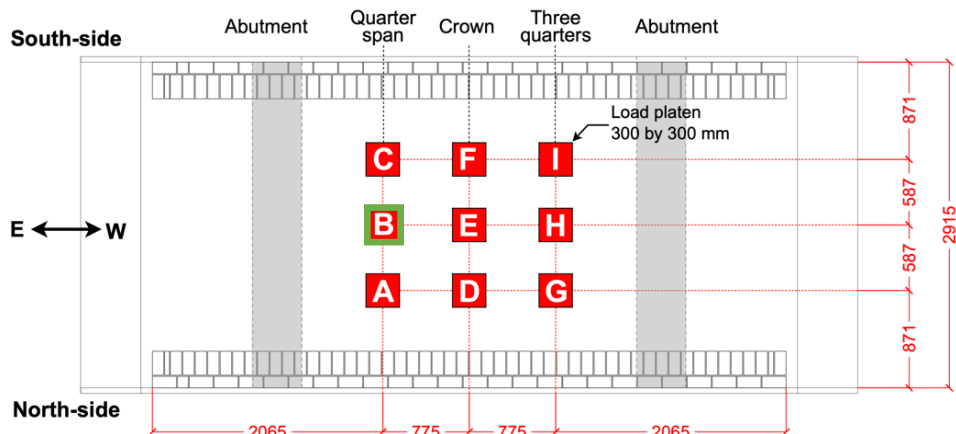


Tensile crack at arch intrados

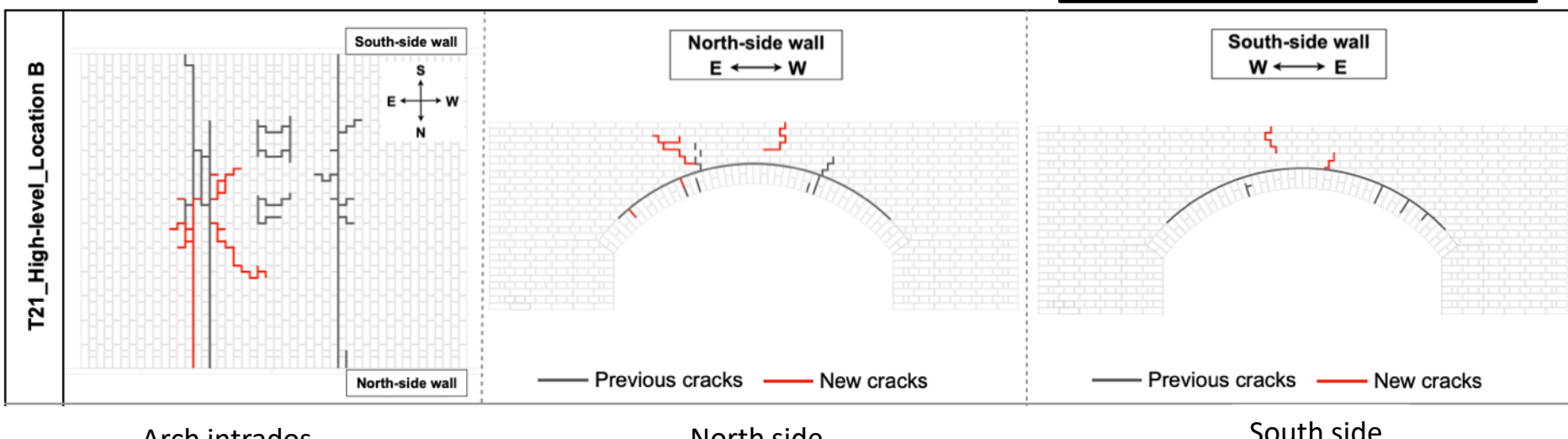
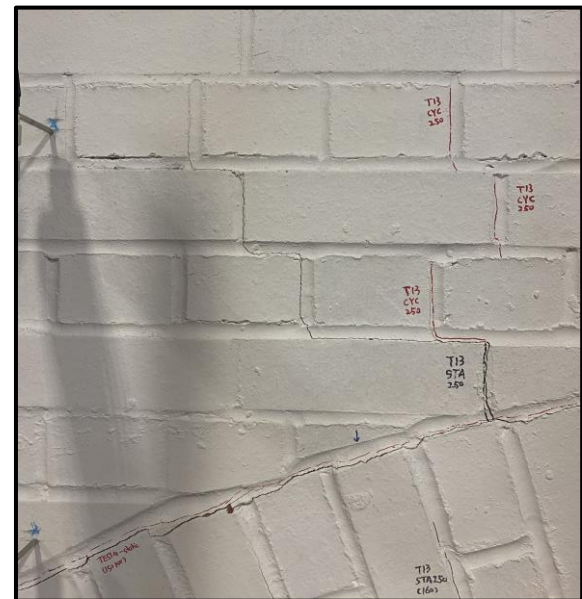


Results: Crack propagation

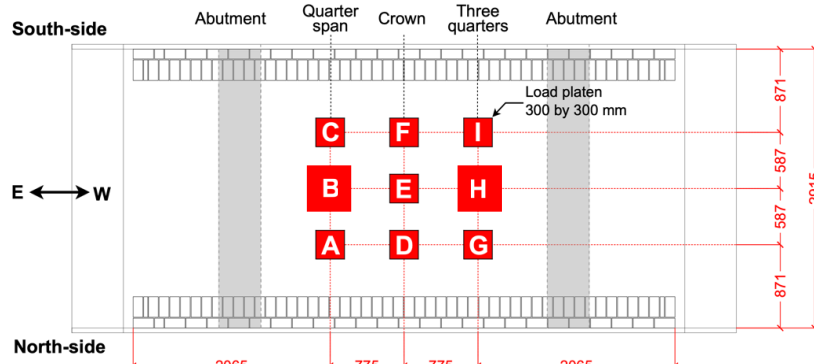
- High-level: 560 kN**



Propagation of diagonal cracks at spandrel wall

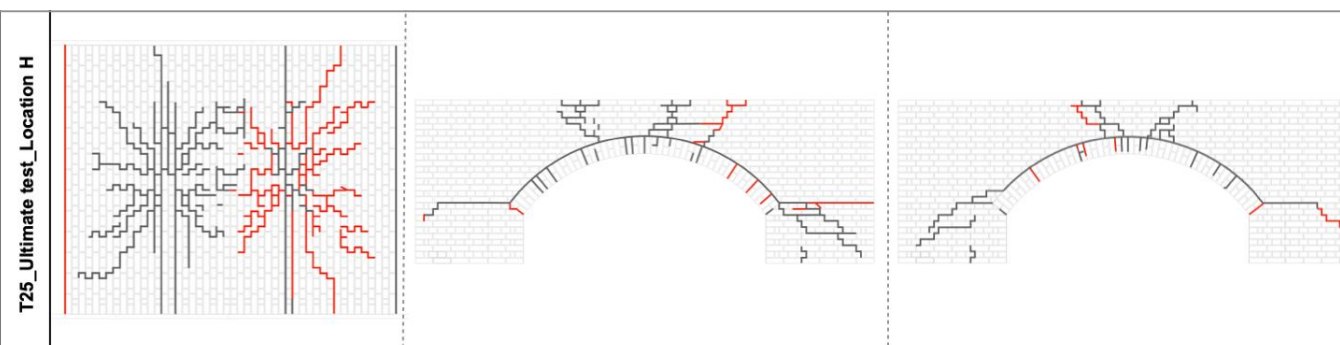
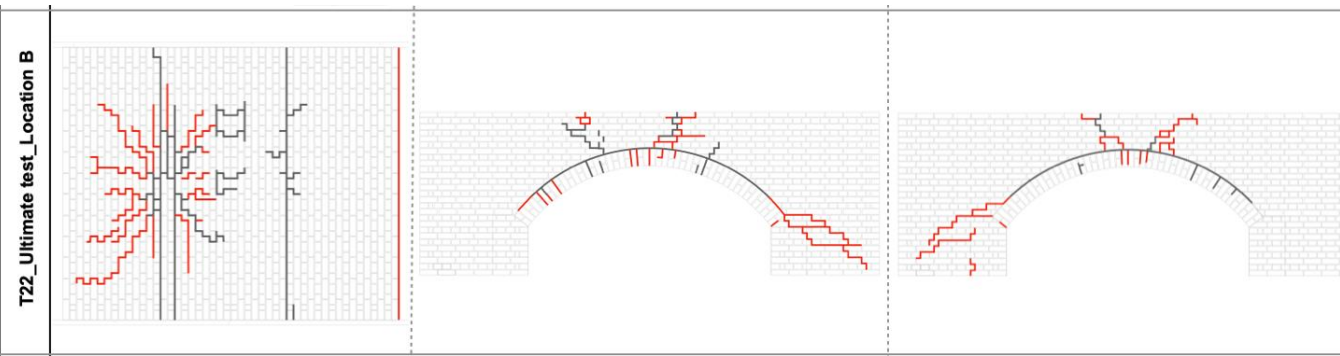


Results: Crack propagation



Failure-level tests

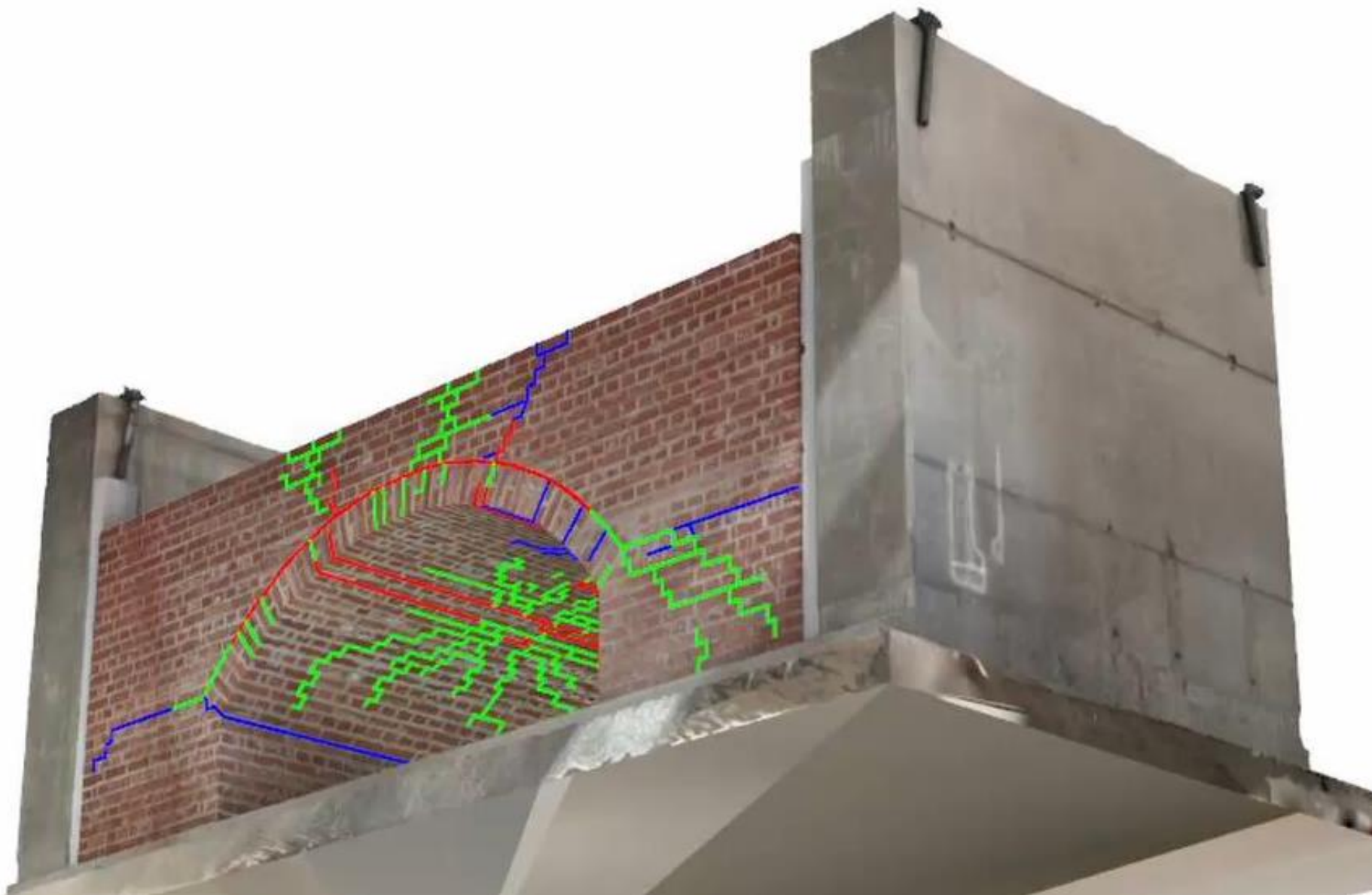
Hinge under loading location



Arch intrados

North side

South side



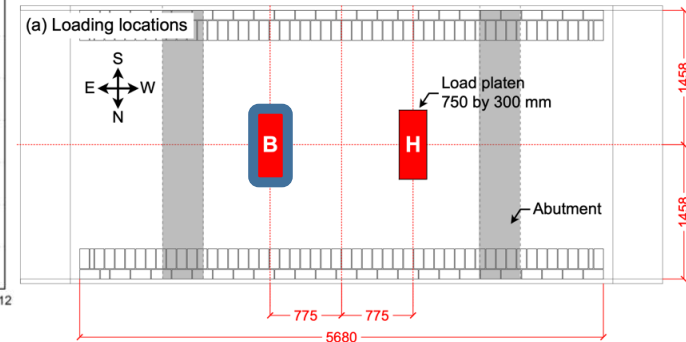
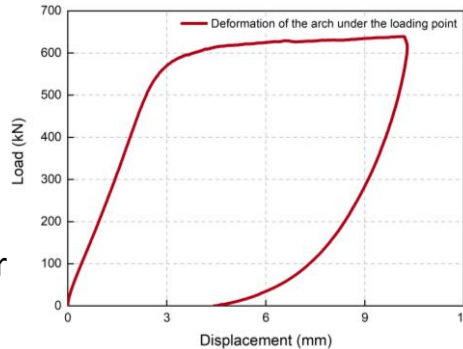
3D Cracking

Results: load vs displacement and bridge failure mechanism

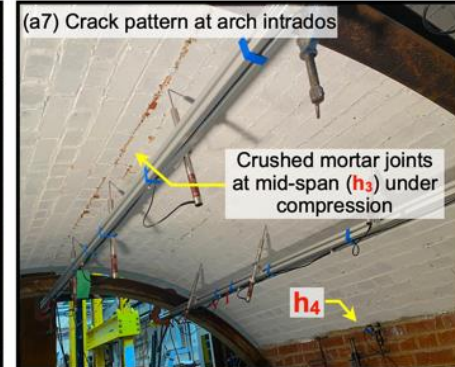
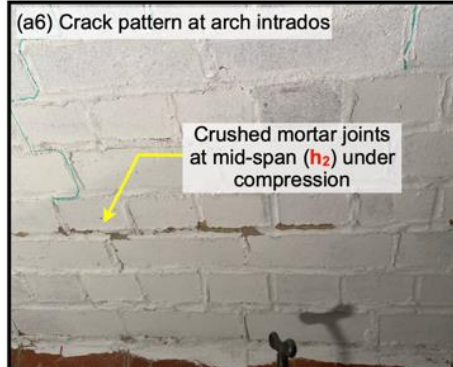
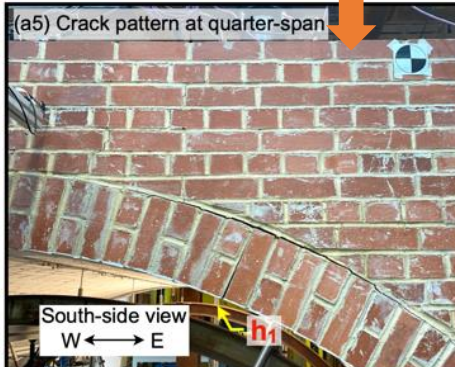
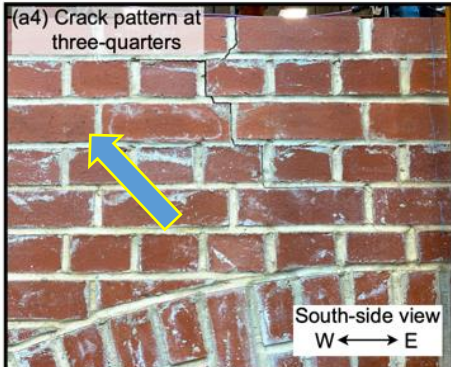
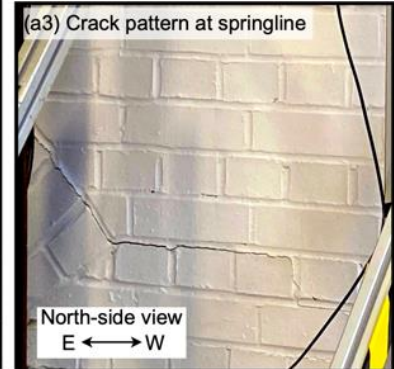
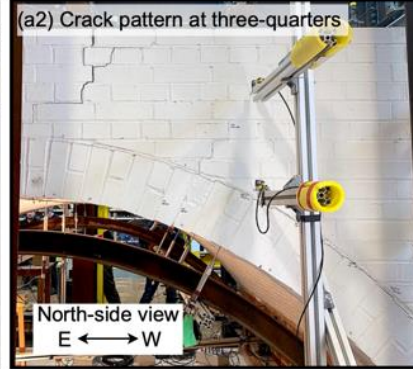
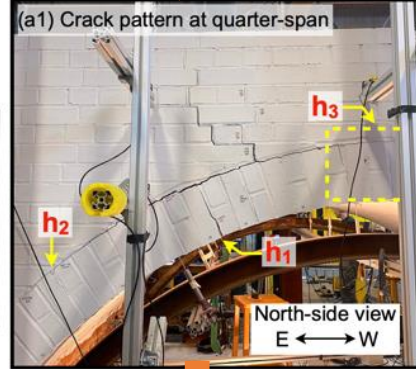
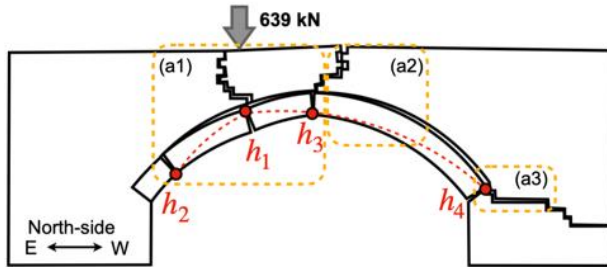


UNIVERSITY OF LEEDS

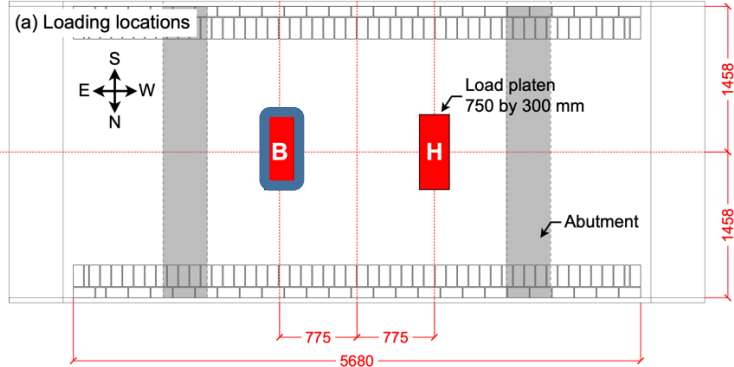
- **Loading location:** Point B
- **Peak load applied:** 639 kN
- **Loading area:** 300 by 750 mm
- **Failure mechanism:** four-hinge behaviour
- Hinge-3 at the mid-span region



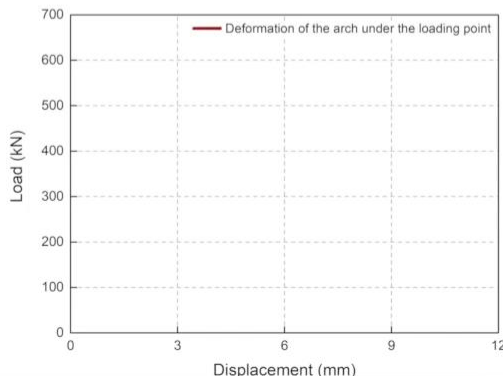
(a) Failure mechanism at T22



Results: Behaviour of the bridge: video recording

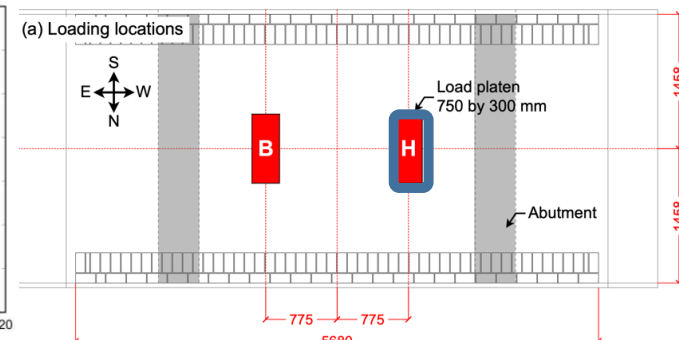
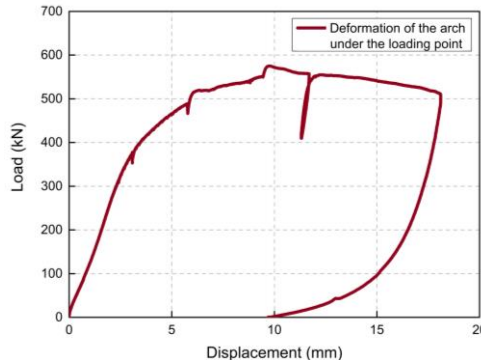


- T22
- 750 by 300 mm platen
- Loading at point B
- South right-hand side wall
- 639kN

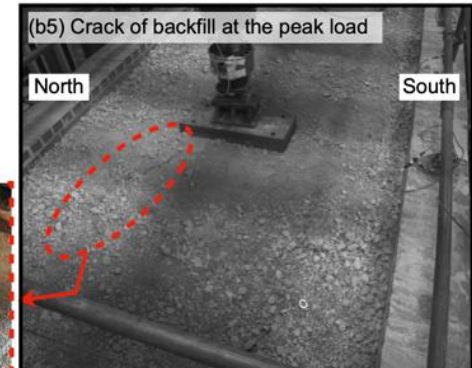
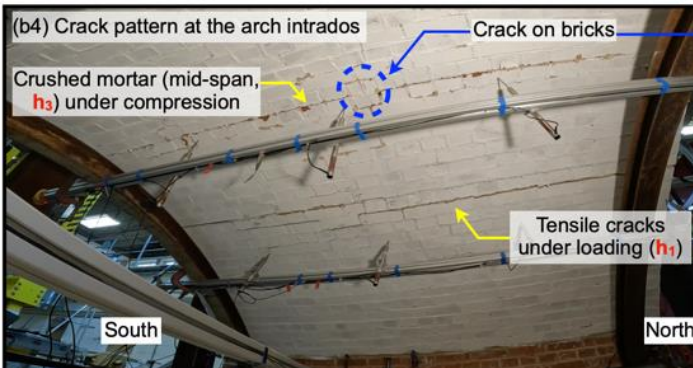
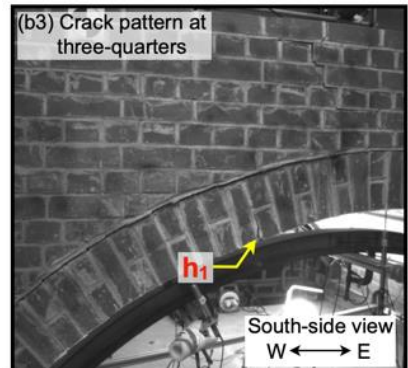
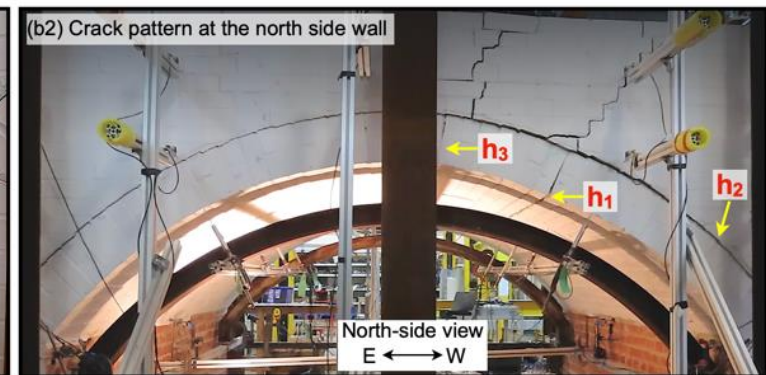
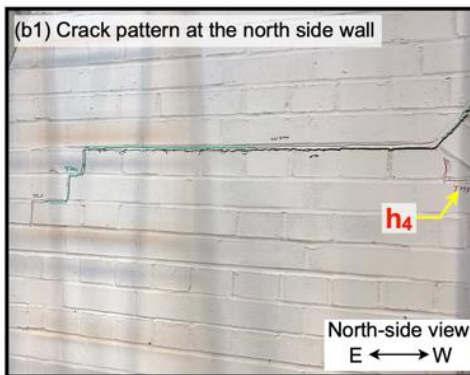
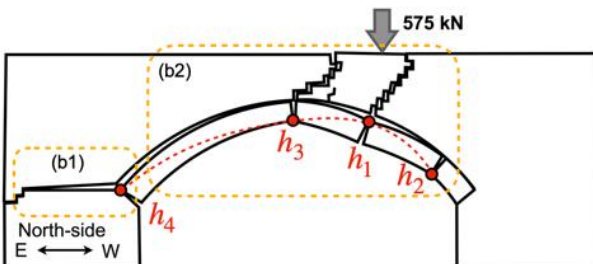


Results: Failure mechanism of the bridge

- **Loading location:** Point H
- **Peak load applied:** 575 kN
- **Loading area:** 300 by 750 mm
- **Failure mechanism:** four-hinge behaviour
- Hinge-3 at the mid-span region
- Diagonal crack observed in backfill



(b) Failure mechanism at T25



Crushing of mortar



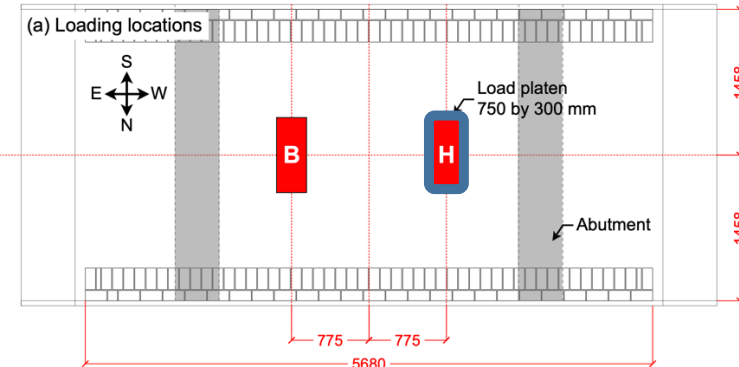
UNIVERSITY OF LEEDS



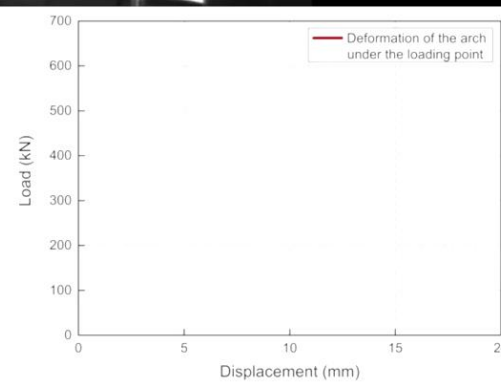
Behaviour of the bridge: video recording

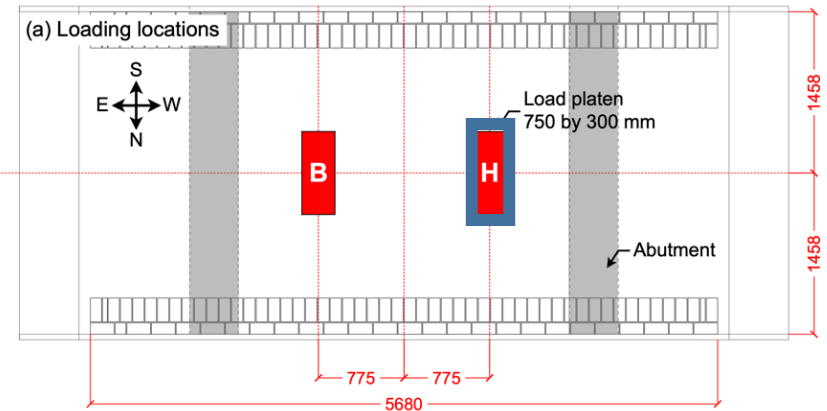


Application of load

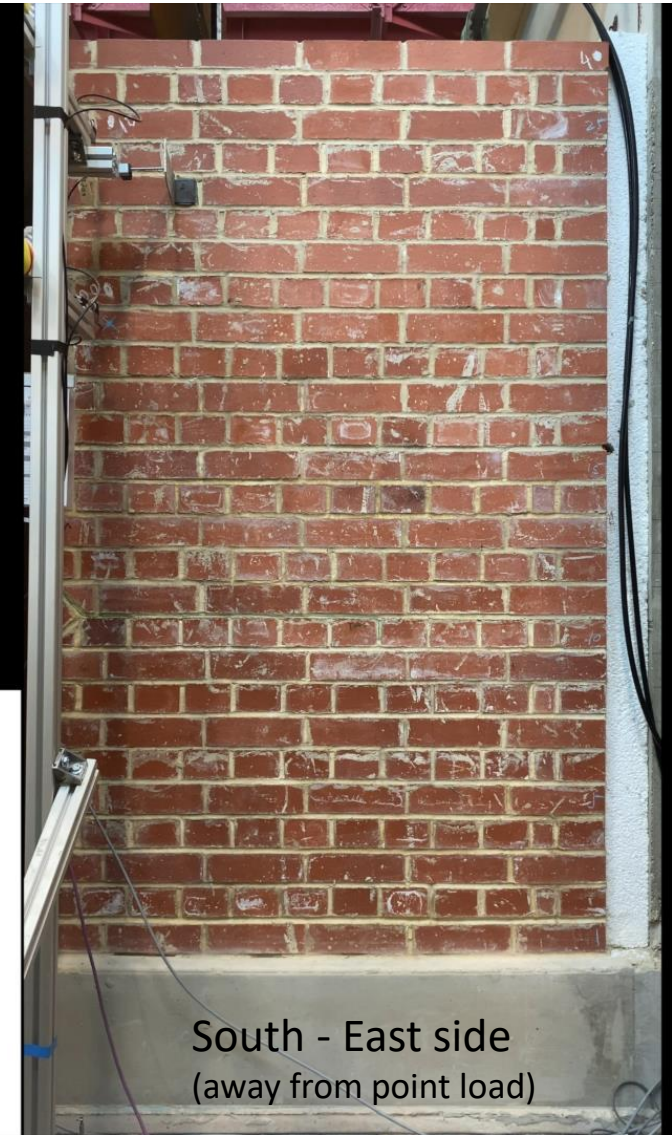
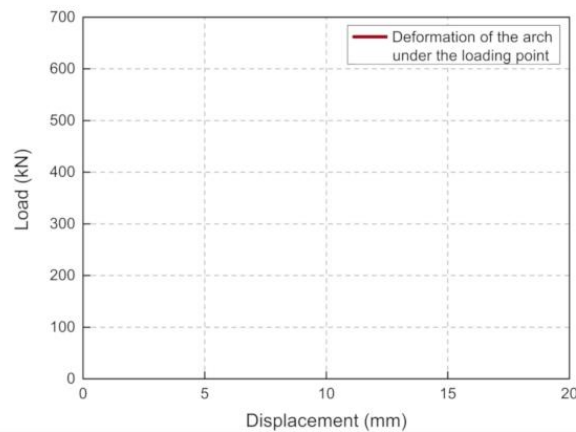
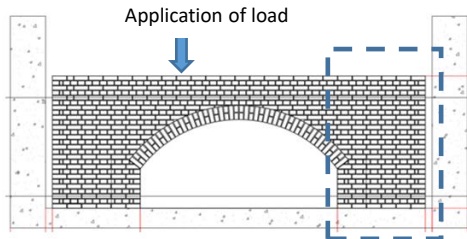
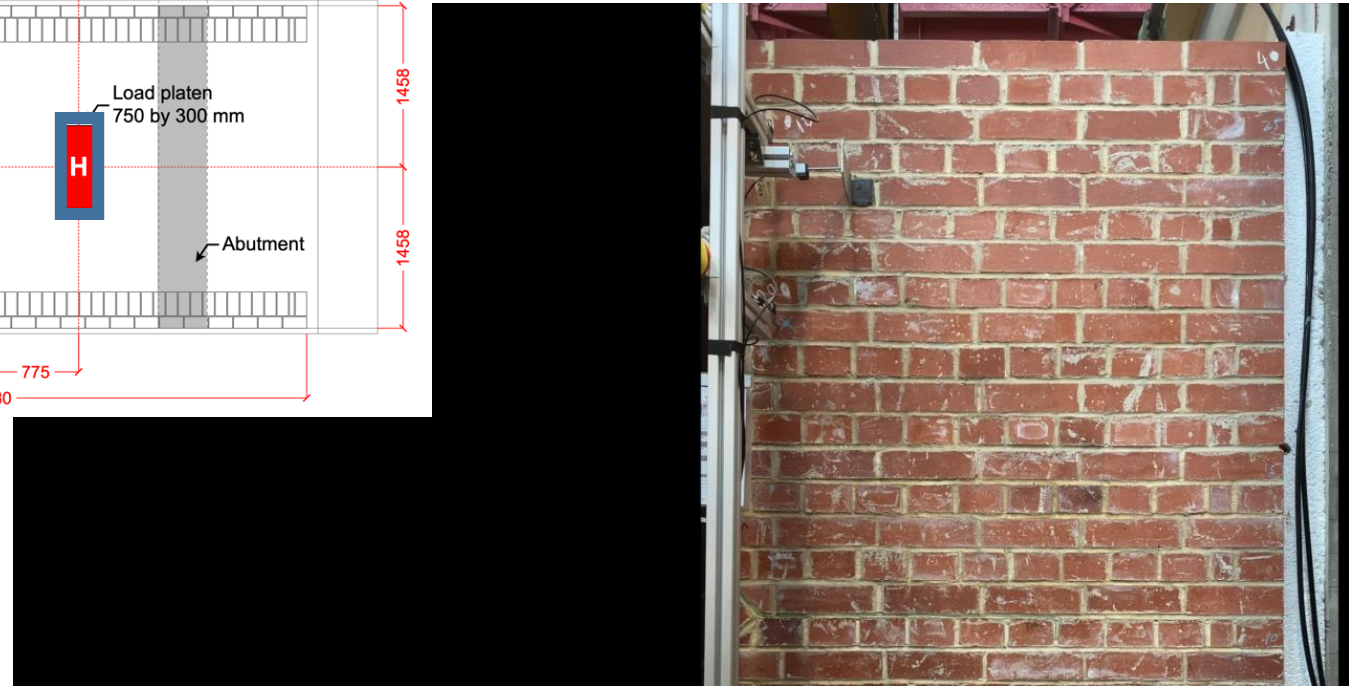


- T25
- 750 by 300 mm platen
- Loading at point H
- South left-side spandrel wall





- T25
- 750 by 300 mm platen
- Loading at point H
- South-right-hand side wall
- 575 kN



Behaviour of the bridge: video recording



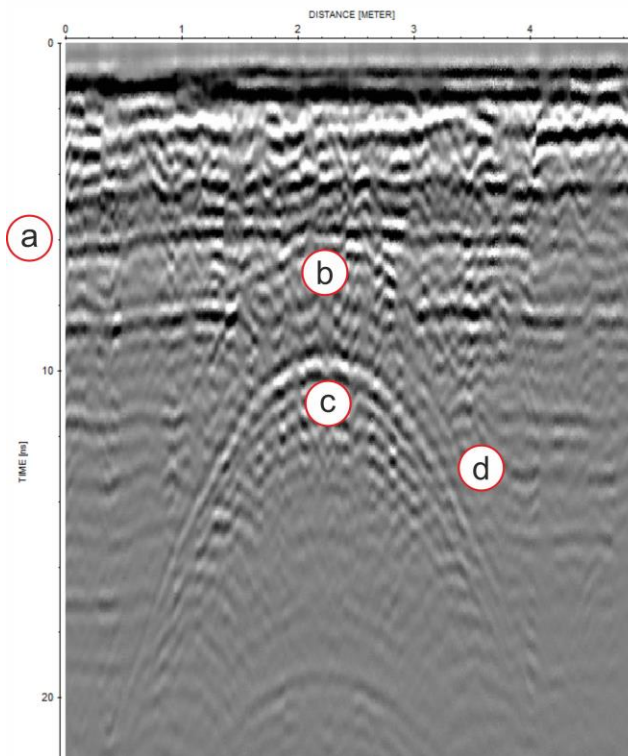
UNIVERSITY OF LEEDS



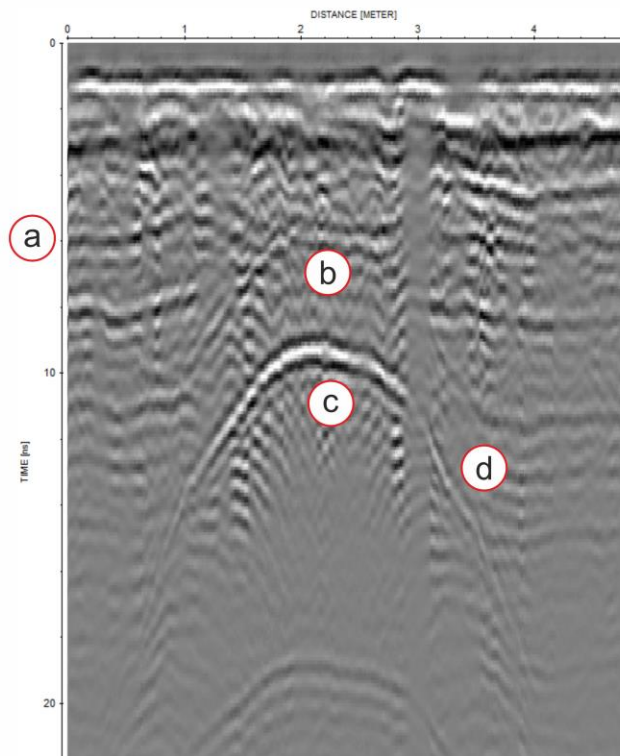


Cracking of backfill

BEFORE DAMAGE



AFTER DAMAGE



- Point a: reflections denote disturbance to the internal layering of the bridge
- Point b: change to the layering immediately above the arch
- Point c: arch rather less symmetrical after the damage,
- Point d: deflections particularly prominent in the flanks.

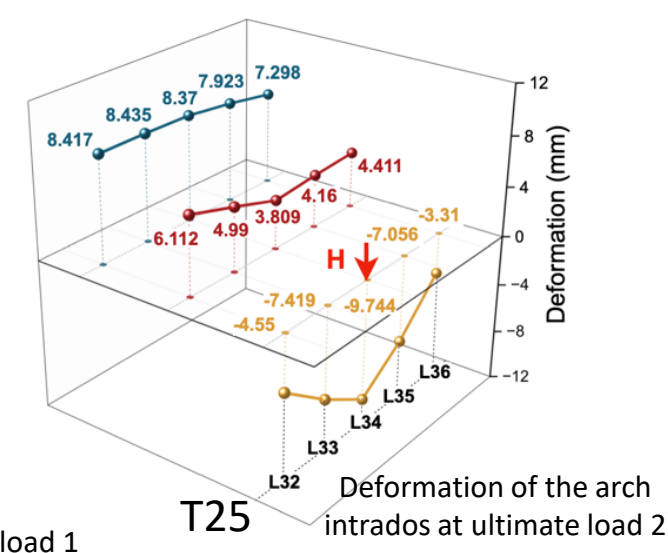
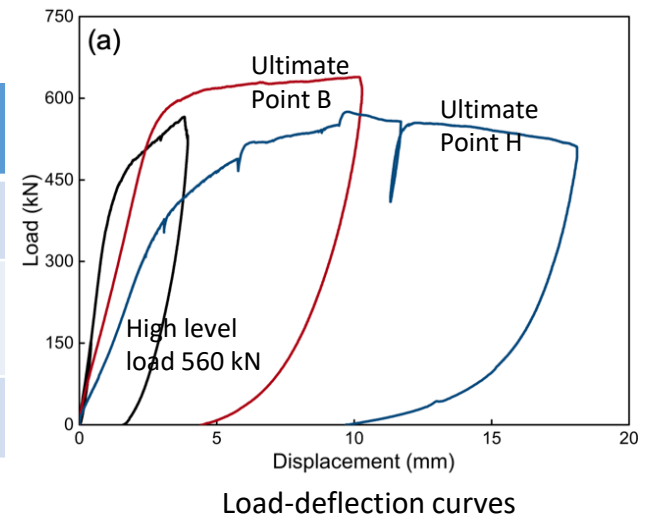
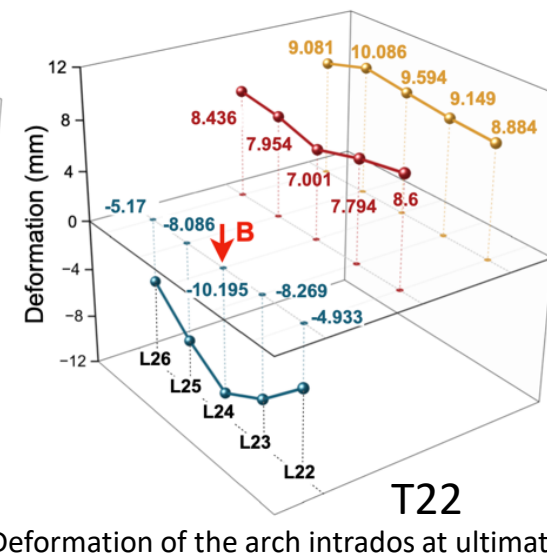
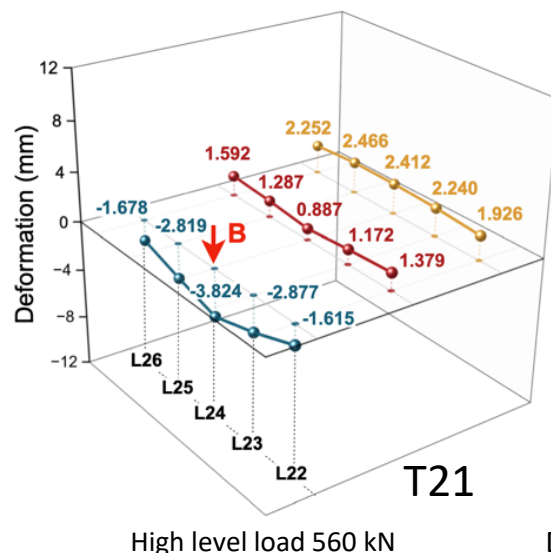
Results: Load-deflection response & stiffness

Load-deformation response during the high-level and ultimate tests

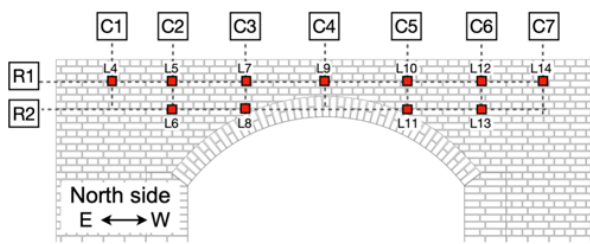
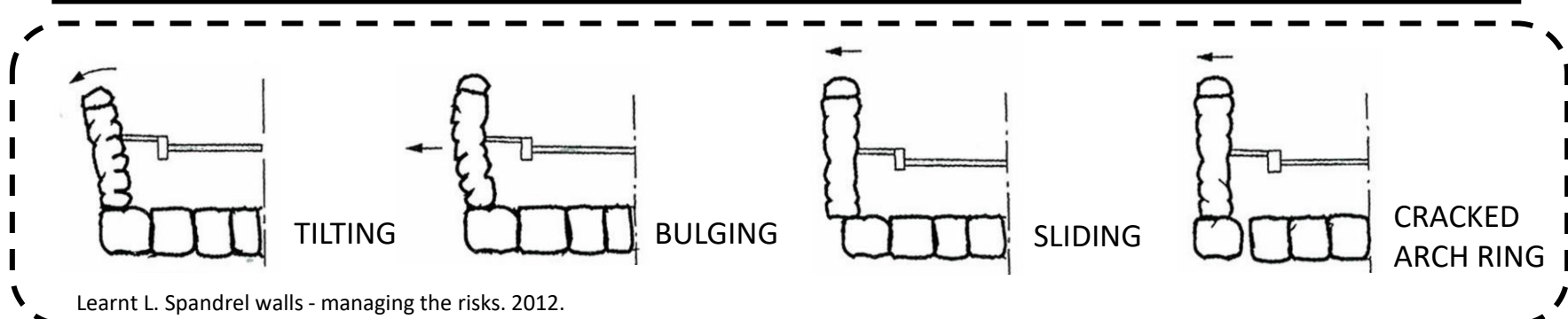
| | T21 (high level) (Point B) | T22 (Ultimate 1) (Point B) | T25 (Ultimate 2) (Point H) |
|-----------------------------------|-------------------------------|-------------------------------|-------------------------------|
| Peak load (kN) | 535 | 639 | 575 |
| Deformation at the peak load (mm) | 3.2 | 10.2 | 7.4 |
| Stiffness* (kN/mm) | 215 | 195 | 127 |

* The values of stiffness were determined by calculating the slope of the load-deflection curve between 10% and 40% of the peak load.

3D response was observed in the arch barrel under patch loading



Results: Peak out-of-plane deformation of spandrel walls



(a) High-level test (T21, Location B)

| | | | | | | | |
|----|------|------|------|------|------|------|------|
| R1 | 0.86 | 0.92 | 0.63 | 0.41 | 0.16 | 0.21 | 0.28 |
| R2 | - | 0.63 | 0.87 | - | 0.22 | 0.2 | - |

C1 C2 C3 C4 C5 C6 C7

(b) Ultimate test; (T22, Location B)

| | | | | | | | |
|----|------|-------|------|------|------|------|-----|
| R1 | 2.59 | 2.34 | 1.9 | 1.87 | 0.54 | 0.3 | 0.7 |
| R2 | - | 1.792 | 2.63 | - | 0.43 | 0.72 | - |

C1 C2 C3 C4 C5 C6 C7

(c) Ultimate test; (T25, Location H)

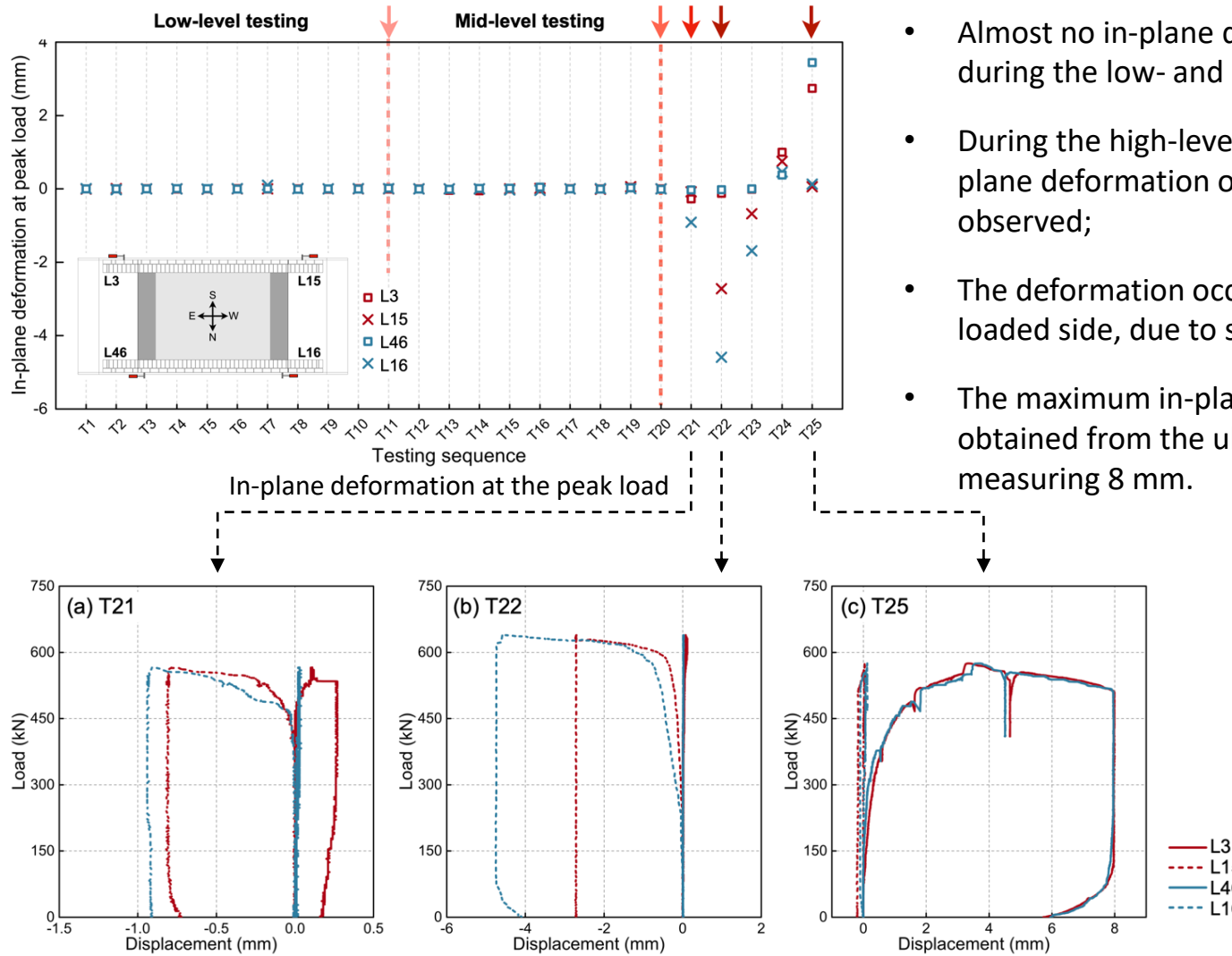
| | | | | | | | |
|----|------|-------|------|------|------|------|------|
| R1 | 0.31 | 0.9 | 0.8 | 2.82 | 5.27 | 3.95 | 4.68 |
| R2 | - | 0.589 | 1.01 | - | 4.73 | 4.81 | - |

C1 C2 C3 C4 C5 C6 C7

Out-of-plane deformation at the peak load (mm)

- When the load applied above the span of the arch, the spandrel walls moved outwards
- Failure mechanism: **combined effects of tilting and sliding**.
- The location closest to the loading had the most significant out-of-plane deformation, as it was subjected to the greatest lateral soil pressure under patch loading.
- Maximum out of plane deformation was approx **1 mm for the high level test, 2.6 mm for the ultimate 1 and 5.3 mm for the ultimate 2**

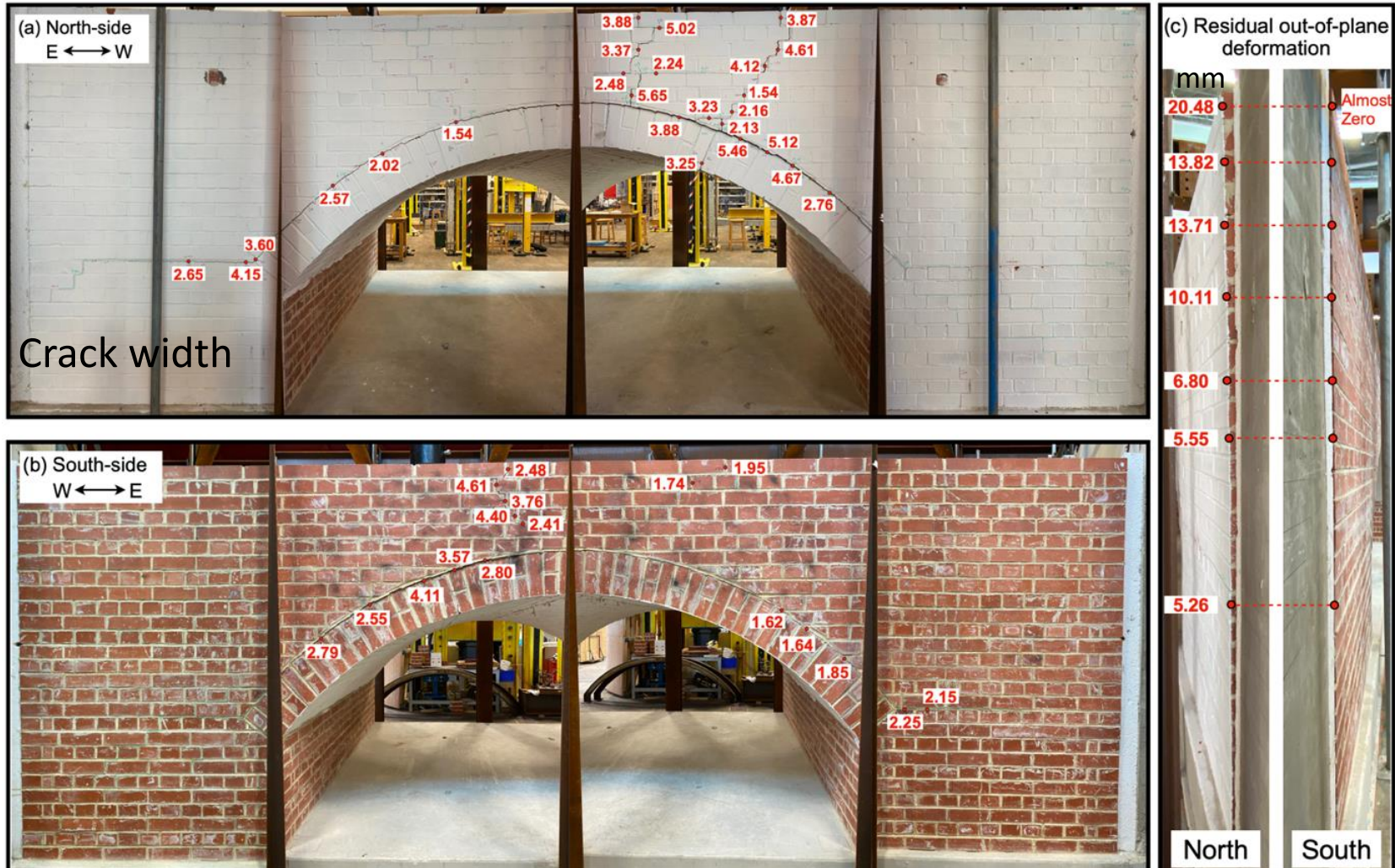
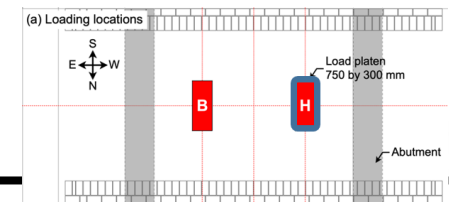
Results: In-plane deformation of spandrel walls



- Almost no in-plane deformation was observed during the low- and mid-level testing;
- During the high-level and ultimate tests, in-plane deformation of the spandrel walls was observed;
- The deformation occurred away from the loaded side, due to sway of the arch barrel.
- The maximum in-plane deformation was obtained from the ultimate test 2 (T25), measuring 8 mm.

Displacement versus in-plane deformation curves for (a) T21, (b) T22, and (c) T25.

Results: Final crack width (after all tests)



- Damage on the north-side wall was more severe (max crack at hinge 5.46 mm)
- The south-side of wall didn't have any noticeable out-of-plane deformation

- A new full-scale testing platform for masonry arch bridges has been developed, incorporating a stiff U-shaped RC test bed.
- A 3m span brickwork arch bridge has been constructed, extensively instrumented and then subjected to a wide range of load tests, culminating in load tests to failure.
- The results obtained from the tests provide a rich dataset that can be used to validate numerical models.
- Specifically, it was found that separation of the spandrel wall and the arch ring before the formation of any visible hinges within the arch ring observed.
- Both fill and spandrel walls contributed to the strength of the bridge.
- Medium and higher magnitude point loads led to 3D modes of response being mobilised, but that when the bridge was loaded to failure, 2D modes of response were observed.
- Even if the bridge reached failure when testing it at quarter span, the bridge could sustain 90% of residual load as evidence when testing it from the opposite $\frac{3}{4}$ span.
- A future test will involve the application of cyclic loading regimes, to more faithfully replicate real-world traffic loads.

Acknowledgements

- Prof. Steve Garrity (Leeds University)
- Prof. Kostas Tsavdaridis (City University)
- Dr Dimitris Loverdos (Leeds University)
- Dr Imrose Muhit (Teesside University)
- Dr Anastasios Drougkas (UPC Barcelona)
- Laboratory technicians at Leeds (Ian Day, Mr Kamran, Mr Marvin William, Mr Rob Clarkson)

- Funding from:



Engineering and
Physical Sciences
Research Council



Questions?